Scalable Cross-View Sample Alignment for Multi-View Clustering with View Structure Similarity

Jun Wang[1] **Zhenglai Li**[2] **Chang Tang**[3] **Suyuan Liu**[1] **Hao Yu**[1] **Chuan Tang**[1]
Miaomiao Li[4*] **Xinwang Liu**[1*]
[1]National University of Defense Technology, Changsha, China
[2]Shenzhen Institutes of Advanced Technology, Shenzhen, China
[3]Huazhong University of Science and Technology, Wuhan, China
[4]Changsha College, Changsha, China

Abstract

Most existing multi-view clustering methods aim to generate a consensus partition across all views, based on the assumption that all views share the same sample arrangement. However, in real-world scenarios, the collected data across different views is often unsynchronized, making it difficult to ensure consistent sample correspondence between views. To address this issue, we propose a scalable sample-alignment-based multi-view clustering method, referred to as SSA-MVC. Specifically, we first employ a cluster-label matching (CLM) algorithm to select the view whose clustering labels best match those of the others as the benchmark view. Then, for each of the remaining views, we construct representations of non-aligned samples by computing their similarities with aligned samples. Based on these representations, we build a similarity graph between the non-aligned samples of each view and those in the benchmark view, which serves as the alignment criterion. This alignment criterion is then integrated into a late-fusion framework to enable clustering without requiring aligned samples. Notably, the learned sample alignment matrix can be used to enhance existing multi-view clustering methods in scenarios where sample correspondence is unavailable. The effectiveness of the proposed SSA-MVC algorithm is validated through extensive experiments conducted on eight real-world multi-view datasets.

1 Introduction

Clustering aims to assign each sample to its corresponding class by leveraging the intrinsic similarities within the original data [1]. With the rapid advancement of science and technology, data have become increasingly diverse in their forms of representation. The same object can often be described from multiple perspectives. For instance, video content can be represented through audio, visual, and textual modalities. Such heterogeneous but complementary data representations are collectively referred to as multi-view data [2, 3, 4, 5]. To fully exploit the rich semantic information embedded in multi-view data, a variety of advanced multi-view clustering algorithms have been developed in recent years [6, 7, 8, 9]. These methods have demonstrated promising performance across a wide range of real-world applications by effectively integrating complementary information from multiple views.

Despite the effectiveness of these approaches in integrating multi-view information, they typically rely on the assumption of strict one-to-one correspondence among samples across different views, which is an idealized condition in practical applications [10, 11, 12]. In real-world scenarios, variations in

*Corresponding Author

39th Conference on Neural Information Processing Systems (NeurIPS 2025).

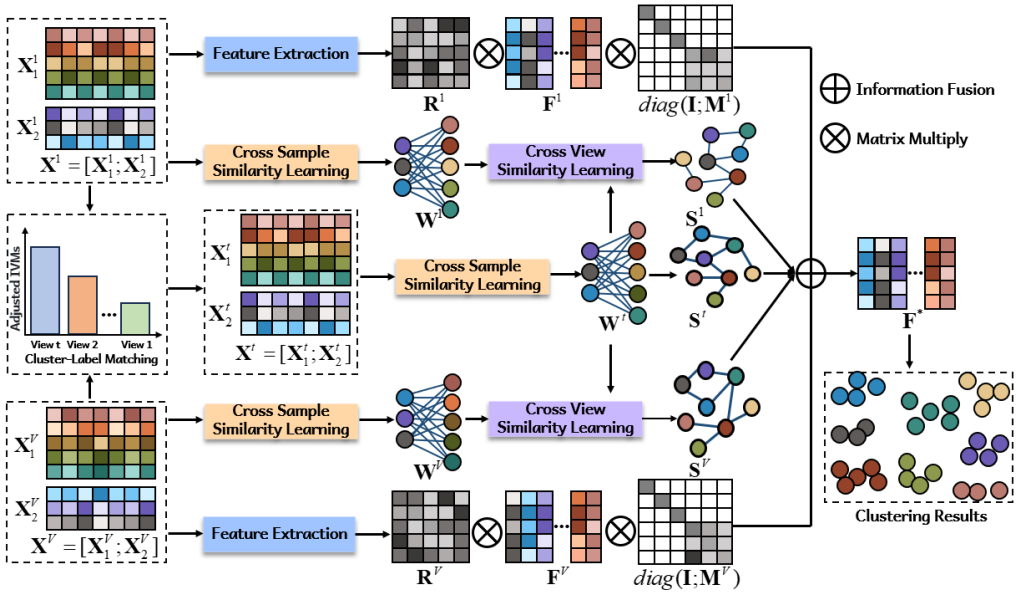

Figure 1: The flowchart of the proposed method. First, the baseline view is selected based on the CLM criterion. Next, feature representations of the unaligned samples, denoted as $\{\mathbf{W}^v\}_{v=1}^V$, are constructed. Subsequently, the cross-view similarity graphs $\{\mathbf{S}^v\}_{v=1}^V$ between the baseline view and the other views are established. Finally, these cross-view similarity graphs serve as alignment constraints within a late fusion multi-view clustering framework to obtain a unified partition matrix $\mathbf{F}^*$. The final clustering results are then derived by applying k-means clustering on $\mathbf{F}^*$.

sample organization or ordering across views commonly lead to inconsistent or misaligned sample correspondences. To this end, some studies attempt to achieve sample alignment jointly with the learning of data representations. Given the effectiveness of the Hungarian algorithm in assignment problems [13], Huang et al. [14] integrated it into their clustering framework to facilitate sample alignment. However, due to semantic discrepancies between views and high intra-class similarity within views, establishing strict one-to-one alignment based solely on sample similarity limits tolerance to noise and misalignment. To address this, Yang et al. [15] proposed alignment at the class level, reformulating it as a class identification problem and introducing a noise-robust contrastive loss to improve robustness. Furthermore, Ren et al. [16] leveraged sample commonality and view diversity to adaptively construct alignment matrices and designed an unsupervised data completion mechanism to handle incomplete or unaligned data.

Although the aforementioned algorithms have shown promising performance in multi-view clustering with sample alignment, they still face several limitations. (1) Due to semantic discrepancies across views and the absence of supervision, establishing strict one-to-one correspondences is often difficult. In real-world scenarios, the sample relationships of different views are typically many-to-many, and enforcing strict matching may introduce noise and lead to sub-optimal alignment [17]. (2) While some recent methods employ joint learning frameworks that integrate alignment with feature representation to enhance performance, they often fail to model explicit alignment relationships, thus limiting their scalability to other multi-view clustering methods that are not applicable in sample non-alignment scenarios [18, 19]. (3) Clustering performance is heavily influenced by the choice of a benchmark view, yet selecting an appropriate one remains an open challenge in current approaches [20].

Therefore, we propose a scalable multi-view clustering algorithm that integrates sample alignment into a unified clustering framework. To mitigate the impact of structurally noisy or disordered views, we first employ the CLM algorithm [21] to select the view that exhibits the highest structural consistency with the underlying semantic labels, designating it as the baseline. Considering that samples within the same subspace can be linearly reconstructed by their peers [22], we reformulate the alignment task as a similarity-based reconstruction problem rather than relying on rigid one-to-one index matching. Specifically, each view is structurally characterized by computing the similarity between unaligned samples and the rest of the view. Then, an alignment relationship is established by comparing these

structural representations to that of the baseline view. Finally, the resulting alignment matrices are incorporated into a late fusion clustering framework, enabling effective alignment without the need for direct correspondence. Furthermore, the learned alignment relationship can be reused as auxiliary information to enhance the performance of existing multi-view clustering methods under misaligned conditions.

Overall, the main contributions of this paper are listed as follows:

- We propose to select the baseline view by measuring the similarity between sample cluster distributions and their corresponding labels within each view, effectively minimizing the impact of irrelevant or noisy structural information on the alignment process.
- We propose a structural representation for each view based on the correlation between non-aligned and aligned samples. This representation guides cross-view alignment by integrating sample-level features with intrinsic structural information.
- An alternating optimization algorithm is proposed to efficiently solve the model. Its effectiveness is validated through extensive experiments on eight multi-view datasets.

2 Preliminaries

2.1 Adaptive Neighbor Graph Learning

Graph-based multi-view clustering algorithms have attracted considerable attention in recent years due to their strong capability in capturing the intrinsic structural information embedded in the original data [23, 24, 25, 26]. Based on the fact that samples within the same cluster or samples with smaller pairwise distances tend to exhibit higher similarity than those from different clusters, Nie et al. [27] proposed a clustering algorithm that constructs a nearest-neighbor graph to capture local structural relationships. The objective function of this method is formulated as follows:

$$\min_{\mathbf{S}} \sum_{i=1}^{n} \sum_{j=1}^{n} \left(\|\mathbf{x}_i - \mathbf{x}_j\|_2^2 \cdot s_{ij} + \beta s_{ij}^2 \right) \quad s.t.\ \mathbf{s}_i^\top \mathbf{1} = 1, 0 \leq s_{ij} \leq 1, \tag{1}$$

where $\mathbf{x}_i$ and $\mathbf{x}_j$ denotes the i-th and j-th samples of the original data matrix $\mathbf{X} \in \mathbb{R}^{n \times d}$, where n is the total number of samples and d is the feature dimension. The variable s_{ij} indicates the similarity between samples $\mathbf{x}_i$ and $\mathbf{x}_j$. The parameter β is a regularization coefficient that balances the trade-off between the similarity graph learning and the sparsity of the graph, and it can be adaptively tuned during the optimization process. For a more detailed description of Eq. (1), please refer to [27].

2.2 Late Fusion based Multi-view Clustering

Given multi-view datasets $\mathbf{X}^v \in \mathbb{R}^{n \times d_v}$, where d_v denotes the feature dimensionality of the v-th view, late fusion-based multi-view clustering methods aim to extract partition-level clustering information from each view. A unified partition matrix is then obtained by integrating the partition information from all views. Specifically, assuming that the base partition matrices $\mathbf{F}^v \in \mathbb{R}^{n \times d_u}$ are obtained from $\mathbf{X}^v$ via eigen-decomposition or other representation learning techniques, where d_u denotes the latent feature dimension, the typical mathematical formulation can be expressed as follows [28]:

$$\max_{\mathbf{F}^*} \Phi(\mathbf{F}^*, \mathbf{F}^v) + \lambda \Psi(\mathbf{F}^*), \tag{2}$$

where $\Phi(\cdot)$ denotes the partition fusion module, which integrates the base partitions into a unified one, and $\Psi(\cdot)$ represents a regularization term designed to preserve desirable properties such as smoothness [29], sparsity [30], or consistency across views [31, 32].

3 Proposed Method

3.1 Cross Sample Similarity Learning

Late fusion-based multi-view clustering algorithms have attracted substantial attention due to their demonstrated effectiveness, and a variety of advanced methods have been proposed within this

framework [33, 34, 35]. However, a common assumption in these algorithms is the existence of a strict one-to-one correspondence between samples across all views during the fusion of partition information. In practice, this assumption is often idealized. Due to temporal misalignment during data acquisition or storage constraints, mismatches between samples across different views frequently occur. Under such circumstances, directly fusion partition-level information without addressing the cross-view sample alignment may introduce irrelevant or inconsistent structural information, thereby degrading the quality of the unified partition and affecting the final clustering performance.

To overcome the limitations of traditional late fusion strategies, several algorithms have introduced a sample alignment matrix jointly with view-specific representation learning, integrating the two processes into a unified framework to enable mutual reinforcement [36, 37, 38]. In the context of unsupervised learning, sample alignment is typically inferred by exploiting the intrinsic feature similarities among data samples. However, due to the presence of substantial cross-view heterogeneity, the assumption of semantic consistency across views is often difficult to capture using rigid one-to-one matching strategies. Such hard alignment approaches fail to model potential one-to-many or many-to-one semantic relationships across views, thereby overlooking alternative and potentially meaningful alignment relationships. Moreover, although some methods attempt to embed the sample alignment process into neural network-based representation learning, they often do not explicitly model the alignment relationships themselves, which limits the scalability of these approaches.

In light of the above challenges, we propose a novel strategy that utilizes the correlation between unaligned and aligned samples within each view as a view-specific structural representation. Specifically, given an unaligned multi-view dataset $\mathbf{X}^v = [\mathbf{X}_1^v; \mathbf{X}_2^v]$, where $\mathbf{X}_1^v \in \mathbb{R}^{n_1 \times d_v}$ and $\mathbf{X}_2^v \in \mathbb{R}^{n_2 \times d_v}$ denote the aligned and unaligned samples in the v-th view, respectively, and where n_1 and n_2 are the corresponding numbers of aligned and unaligned samples, we construct the structural representations of the unaligned samples for each view based on Eq. (1), i.e.,

$$\min_{\{\mathbf{W}^v\}_{v=1}^V} \sum_{v=1}^{V} \sum_{i=1}^{n_2} \sum_{j=1}^{n_1} \left\| \mathbf{X}_{1[i,:]}^v - \mathbf{X}_{2[j,:]}^v \right\|_2^2 w_{ij}^v + \beta \left(w_{ij}^v\right)^2 \quad s.t.\ \mathbf{w}_i^{v\top} \mathbf{1} = 1, 0 \leq w_{ij}^v \leq 1, \tag{3}$$

where V denotes the total number of views. The matrix $\mathbf{W}^v \in \mathbb{R}^{n_2 \times n_1}$ represents the constructed feature representation for the v-th view in the presence of sample non-alignment. It is worth noting that the above construction of the feature representation for each view is not unique. Here we adopt the formulation given in Eq. (1) for simplicity. Nevertheless, alternative learning mechanisms could also be employed within our framework.

3.2 Cross View Similarity Learning

After obtaining the feature representations for all views, a key challenge lies in constructing a reliable sample alignment across views. A straightforward approach is to randomly select one view as the baseline and align the remaining views to it. However, due to inevitable noise introduced during data collection, some views may contain structural information that does not reflect the true underlying cluster distribution. To mitigate the impact of such irrelevant or misleading information on the alignment process, we adopt the CLM algorithm to identify the most reliable baseline view. Specifically, the view that exhibits the highest consistency between its sample distribution structure and the semantic labels is selected as the baseline. The detailed selection process is defined as:

$$H(Y, \mathbf{X}, d^2) = \frac{\exp\left(\frac{1}{\sigma_{d^2} n} \sum_{\mathbf{x} \in \mathbf{X}} d^2(\mathbf{x}, y)\right)}{\exp\left(\frac{1}{\sigma_{d^2} n} \sum_{i=1}^{k} \sum_{\mathbf{x} \in Y_i} d^2(\mathbf{x}, y_i)\right)} \times \frac{\sum_{i=1}^{k} |Y_i| d^2(y_i, y)}{\sigma_{d^2}\, n\, (k-1)} \tag{4}$$

$$CLM(\mathbf{X}) = \frac{1}{2\binom{k}{2}} \sum_{\substack{G \subseteq Y \\ |G|=2}} \frac{1}{1 + \exp\left(-\delta \cdot H(G, \mathbf{X}, d^2)\right)} \tag{5}$$

where $Y = \{Y_1, Y_2, \cdots, Y_k\}$ denotes the ground-truth cluster assignment of the dataset $\mathbf{X}$, and k is the total number of clusters. Let $y_i = \overline{Y_i}$ denote the mean of the samples in the i-th cluster, and $c = \overline{\mathbf{X}}$ denote the mean of all samples. The function $d^2(\cdot)$ represents the squared Euclidean distance, and $\sigma_{d^2} = std(d^2(x, c) | \mathbf{x} \in \mathbf{X})$ denotes the standard deviation of the distances between the original data samples and the global centroid. The parameter δ is a pre-defined scaling factor. Based on

the above formulation, we compute a matching score that quantifies the consistency between the structural distribution of samples and the corresponding semantic clusters in each view. The view with the highest matching score is then selected as the baseline. Accordingly, the cross-view structural similarity graph $\mathbf{S}^v$ is constructed as follows:

$$\min_{\mathbf{S}^v} \sum_{\substack{v=1 \\ v \neq t}}^{V} \|\mathbf{w}_i^t - \mathbf{w}_j^v\|_2^2 s_{ij}^v + \beta (s_{ij}^v)^2 \quad s.t.\ t = \arg\max_v CLM(\mathbf{X}^v), \mathbf{s}_i^\top \mathbf{1} = 1, 0 \leq s_{ij}^v \leq 1, \tag{6}$$

where $\mathbf{S}^v$ denotes the similarity graph that captures the structural correspondence between the unaligned samples in the v-th view and those in the baseline view, denoted by t. As a special case, when $v = t$, we define the similarity graph as the identity matrix, i.e., $\mathbf{S}^t = \mathbf{I}$.

3.3 Sample-Aligned Late Fusion Strategy

In general, a higher similarity between samples implies a greater likelihood of a semantic match. Based on this intuition, we propose to capture the matching criterion between unaligned samples across views by leveraging cross-view sample similarity. As discussed earlier, the ideal scenario assumes a strict one-to-one correspondence between samples across views. However, in practice, such hard 0-1 alignments are difficult to establish in the absence of external supervision, due to the presence of noise and structurally irrelevant information in certain views.

To address this challenge, we reformulate the alignment problem by reconstructing unaligned samples using samples within their corresponding subspace, rather than explicitly matching index positions across views. In this way, the alignment is achieved in a soft and structure-preserving manner. By integrating this alignment strategy with the late fusion-based multi-view clustering framework, we formulate the final objective function as follows:

$$\begin{aligned} &\max_{\mathbf{R}^v, \mathbf{F}^*, \mathbf{M}^v, \alpha_v} \operatorname{Tr}\left(\mathbf{F}^{*\top}\left(\alpha_t \mathbf{F}^t \mathbf{R}^t + \sum_{\substack{v=1 \\ v \neq t}}^{V} \alpha_v \begin{bmatrix} \mathbf{I} & \mathbf{0} \\ \mathbf{0} & \mathbf{M}^v \end{bmatrix} \mathbf{F}^v \mathbf{R}^v\right)\right) + \lambda \sum_{v=1}^{V} \operatorname{Tr}(\mathbf{M}^{v\top} \mathbf{S}^v) \\ &s.t.\ t = \arg\max_v CLM(\mathbf{X}^v), \mathbf{F}^{*\top}\mathbf{F}^* = \mathbf{I}, \mathbf{R}^{v\top}\mathbf{R}^v = \mathbf{I}, \sum_{v=1}^{V} \alpha_v^2 = 1, \mathbf{M}^{v\top}\mathbf{M}^v = \mathbf{I}, \end{aligned} \tag{7}$$

where $\mathbf{M}^v$ denotes the sample realignment matrix that maps the unaligned samples in the v-th view to those in the baseline view, while $\mathbf{R}^v$ represents the feature rotation matrix used to align the feature space. The scalar α_v indicates the weight assigned to the v-th view, and λ is a hyperparameter that controls the trade-off between feature information and structural information.

4 Optimization

4.1 Optimization Algorithms

In this section, we develop an iterative optimization algorithm to solve the objective function in Eq. (7) with respect to the variables $\mathbf{R}^v$, $\mathbf{F}^*$, $\mathbf{M}^v$, and α_v. The detailed optimization procedure is described as follows:

Update $\mathbf{F}^*$: When optimizing $\mathbf{F}^*$ while keeping all other variables fixed, the objective function in Eq. (7) can be equivalently reformulated as:

$$\max_{\mathbf{F}^*} \sum_{v=1}^{V} \operatorname{Tr}\left(\alpha_v \mathbf{F}_1^{*\top} \mathbf{F}_1^v \mathbf{R}^v + \alpha_v \mathbf{F}_2^{*\top} \mathbf{M}^v \mathbf{F}_2^v \mathbf{R}^v\right) \quad s.t.\ \mathbf{F}^{*\top}\mathbf{F}^* = \mathbf{I}, \mathbf{F}^* = \begin{bmatrix} \mathbf{F}_1^* \\ \mathbf{F}_2^* \end{bmatrix}. \tag{8}$$

Since $\mathbf{F}_1^*$ and $\mathbf{F}_2^*$ are independent of each other, they can be optimized separately to obtain the complete solution for $\mathbf{F}^*$. Specifically, when optimizing the variable $\mathbf{F}_1^*$, the objective function in Eq. (8) can be equivalently rewritten as:

$$\max_{\mathbf{F}_1^*} \sum_{v=1}^{V} \operatorname{Tr}(\mathbf{F}_1^{*\top} \alpha_v \mathbf{F}_1^v \mathbf{R}^v) \quad s.t.\ \mathbf{F}_1^{*\top}\mathbf{F}_1^* = \mathbf{I}. \tag{9}$$

The optimal solution to Eq. (9) can be obtained by performing singular value decomposition (SVD) on the matrix $\alpha_v \mathbf{F}_1^v \mathbf{R}^v$. Since the optimization of $\mathbf{F}_2^v$ follows a procedure analogous to that of $\mathbf{F}_1^v$, we omit the details here for brevity. Once the optimal solutions for both $\mathbf{F}_1^v$ and $\mathbf{F}_2^v$ are obtained, the final solution for $\mathbf{F}^*$ is constructed by concatenating the two parts.

Update $\mathbf{R}^v$: When all other variables are fixed, the optimization of $\mathbf{R}^v$ in Eq. (7) can be equivalently reformulated as:

$$\max_{\mathbf{R}^v} \alpha_v \operatorname{Tr}\left(\mathbf{R}^{v\top}\mathbf{F}^{v\top}\begin{bmatrix}\mathbf{I} & \mathbf{0}\\ \mathbf{0} & \mathbf{M}^v\end{bmatrix}\mathbf{F}^*\right) \quad s.t.\ \mathbf{R}^{v\top}\mathbf{R}^v = \mathbf{I}. \tag{10}$$

Let $\mathbf{Q}^v = \alpha_v \mathbf{F}^{v\top}\begin{bmatrix}\mathbf{I} & 0\\ 0 & \mathbf{M}^v\end{bmatrix}\mathbf{F}^*$, the optimal solution for the variable $\mathbf{R}^v$ can then be obtained like that of $\mathbf{F}_1^*$, specifically by performing singular value decomposition on $\mathbf{Q}^v$.

Update α_v: By fixing other variables, the Eq. (7) can be formulated as:

$$\max_{\boldsymbol{\alpha}} \quad \sum_{v=1}^{V} \alpha_v \gamma_v \quad s.t.\ \sum_{v=1}^{V} \alpha_v^2 = 1, \tag{11}$$

where $\gamma_v = \operatorname{Tr}(\mathbf{F}^{*\top}\mathbf{C}^v\mathbf{F}^v\mathbf{R}^v)$. According to the Cauchy inequality, the optimal solution to the above optimization problem can be derived in closed form as:

$$\alpha_v = \frac{\gamma_v}{\sqrt{\sum_{v=1}^{V}\gamma_v^2}}. \tag{12}$$

Update $\mathbf{M}^v$: By fixing $\mathbf{F}^*$, $\mathbf{R}^v$, and α_v, $\mathbf{M}^v$ can be optimized by solving the following subproblem:

$$\max_{\mathbf{M}^v} \alpha_v \operatorname{Tr}\big(\mathbf{M}^{v\top}\mathbf{F}_2^*\mathbf{R}^{v\top}\mathbf{F}_2^{v\top}\big) + \lambda \operatorname{Tr}\big(\mathbf{M}^{v\top}\mathbf{S}^v\big) \quad s.t.\ \mathbf{M}^{v\top}\mathbf{M}^v = \mathbf{I}. \tag{13}$$

Let $\mathbf{T} = \alpha_v \mathbf{F}_2^* \mathbf{R}^{v\top}\mathbf{F}_2^{v\top} + \lambda \mathbf{S}^v$. Following an optimization procedure similar to that for the variable $\mathbf{M}^v$, the optimal solution can be obtained by performing SVD on the matrix $\mathbf{T}$.

In summary, the detailed procedure of the proposed method is described in the Appendix A.2.

4.2 Convergence Property

In the above optimization process, each subproblem is independent, and its corresponding optimal solution can be obtained. Consequently, the proposed algorithm converges within a few iterations according to Theorem 1. A detailed convergence proof is provided in the Appendix A.3.

Theorem 1. *The proposed optimization algorithm is guaranteed to converge to a local optimum of the SSA-MVC method.*

4.3 Computational Complexity Analysis

In the proposed method, the primary computational complexity arises from three components: cross-sample similarity learning, cross-view similarity learning, and sample-aligned late fusion. Specifically, the computational cost for obtaining the feature representations $\{\mathbf{W}^v\}_{v=1}^V \in \mathbb{R}^{n_2 \times n_1}$ is $\mathcal{O}(Vn_2Kd_{max})$, where K denotes the number of neighbors and $d_{max} = \max\{d_1, d_2, \cdots, d_V\}$ represents the maximum feature dimension across all views. For the CLM algorithm, the complexity is $\mathcal{O}(nd_{max})$, while the construction of the cross-view similarity graph requires $\mathcal{O}(Vn_2n_1K)$ operations. Finally, the computational cost of the late fusion step is $\mathcal{O}(n^2)$, mainly due to the generation of the partition matrix $\mathbf{F}^v$. Consequently, the overall computational complexity is $\mathcal{O}(n^2)$.

5 Experiments

5.1 Datasets

To further validate the effectiveness of the proposed method, we conduct experiments on eight real-world multi-view datasets, including Yale, 3sources, MSRCV, 100leaves, HW, Scene, EMNIST, and Hdigit. The detailed summary of them is provided in Appendix A.4.

Table 1: ACC comparison of all methods with and without Hungarian alignment on eight multi-view datasets under a sample alignment ratio $\rho = 50\%$.

Method	Yale	3sources	MSRCV	100leaves	HW	Scene	EMNIST	Hdigit
EEOMVC	58.18±0.00	59.76±0.00	**72.86±0.00**	65.44±0.00	**93.85±0.00**	26.91±0.00	46.11±0.00	65.93±0.00
EEOMVC + Hungarian	52.73±0.00	48.52±0.00	71.90±0.00	**67.19±0.00**	67.30±0.00	26.00±0.00	44.24±0.00	62.28±0.00
DealMVC	33.94±0.00	31.01±0.00	28.10±0.00	7.69±0.00	47.94±0.00	22.54±0.00	45.62±0.00	65.66±0.00
DealMVC + Hungarian	24.85±0.00	29.11±0.00	28.29±0.00	9.34±0.00	39.97±0.00	21.86±0.00	37.83±0.00	**82.72±0.98**
MVCAN	32.48±2.50	31.12±2.31	58.14±1.76	49.51±1.24	50.62±0.42	**33.30±0.41**	45.06±1.02	65.50±2.98
MVCAN + Hungarian	33.09±1.56	49.37±4.60	51.20±2.80	40.71±1.53	47.08±3.56	29.75±0.54	49.56±9.49	57.37±3.76
EBMGC	39.39±0.00	38.46±0.00	42.86±0.00	33.94±0.00	56.75±0.00	21.58±0.00	33.50±0.00	50.91±0.00
EBMGC + Hungarian	32.73±0.00	40.24±0.00	47.14±0.00	33.94±0.00	51.70±0.00	26.33±0.00	41.00±0.00	59.46±0.00
Vsc_mH	53.94±0.00	**62.13±0.00**	64.29±0.00	38.56±0.00	42.50±0.00	28.03±0.00	46.47±0.00	65.19±0.00
OpVuC	53.94±0.00	57.40±0.00	30.00±0.00	53.13±0.00	30.10±0.00	31.82±0.00	51.09±0.00	62.90±0.00
DCMVC	27.15±1.01	46.51±4.52	45.71±2.29	48.83±0.83	69.34±1.01	26.02±0.60	**59.55±3.60**	65.74±2.31
DCMVC + Hungarian	23.88±1.19	35.15±1.10	44.57±2.46	39.34±0.95	50.47±0.99	24.07±0.45	40.11±1.28	35.80±0.99
LMTC	52.58±3.76	48.28±3.49	53.29±3.15	35.58±0.94	64.99±1.16	28.96±0.92	41.91±0.80	59.25±0.30
LMTC + Hungarian	54.61±4.74	48.05±1.18	55.43±3.29	35.30±1.45	54.24±2.72	28.53±0.86	41.69±0.70	55.46±2.13
TMSL	24.82±1.70	42.25±2.66	43.98±0.97	47.47±1.40	62.61±0.61	29.13±0.49	OOM	OOM
TMSL + Hungarian	**68.79±2.78**	56.21±1.05	44.45±1.45	47.12±1.11	53.12±0.05	27.02±0.24	OOM	OOM
DSTL	35.91±1.93	61.54±0.00	39.48±3.81	36.87±1.42	47.61±1.57	20.45±0.59	28.87±0.40	40.90±0.68
DSTL + Hungarian	37.73±2.76	59.76±0.19	43.71±1.43	30.57±1.03	43.33±0.51	19.31±0.79	30.36±0.33	50.09±0.00
Ours	**64.24±3.62**	**64.44±1.29**	**83.52±0.39**	**70.63±1.29**	**96.55±0.00**	**35.91±0.27**	**77.38±3.14**	**71.78±1.26**

Table 2: NMI comparison of all methods with and without Hungarian alignment on eight multi-view datasets under a sample alignment ratio $\rho = 50\%$.

Method	Yale	3sources	MSRCV	100leaves	HW	Scene	EMNIST	Hdigit
EEOMVC	62.23±0.00	39.32±0.00	56.08±0.00	75.62±0.00	**88.20±0.00**	16.59±0.00	32.54±0.00	**70.96±0.00**
EEOMVC + Hungarian	57.37±0.00	31.87±0.00	**56.93±0.00**	77.03±0.00	62.65±0.00	18.26±0.00	29.18±0.00	53.11±0.00
DealMVC	38.08±0.00	6.69±0.74	14.00±3.92	25.34±0.44	27.20±0.89	11.89±1.09	31.39±0.59	39.90±1.52
DealMVC + Hungarian	23.65±0.00	7.31±0.48	13.08±0.17	27.34±3.63	26.08±2.49	16.31±3.23	22.80±0.48	65.46±1.81
MVCAN	38.43±1.87	12.87±1.67	46.19±1.94	69.50±0.95	32.31±0.48	**30.96±0.89**	20.14±0.13	60.89±1.68
MVCAN + Hungarian	38.53±1.22	47.72±3.00	35.16±4.14	62.08±1.45	45.05±5.03	25.76±0.33	37.94±15.14	53.82±3.54
EBMGC	43.31±0.00	23.68±0.00	22.79±0.00	58.22±0.00	35.99±0.00	11.14±0.00	17.99±0.00	25.07±0.00
EBMGC + Hungarian	38.18±0.00	23.98±0.00	24.79±0.00	58.22±0.00	29.52±0.00	15.08±0.00	19.44±0.00	39.70±0.00
Vsc_mH	62.00±0.00	**48.81±0.00**	56.01±0.00	68.53±0.00	30.67±0.00	25.41±0.00	36.92±0.00	55.77±0.00
OpVuC	55.77±0.00	36.86±0.00	13.63±0.00	**78.00±0.00**	17.74±0.00	29.69±0.00	45.94±0.00	47.51±0.00
DCMVC	31.40±1.27	26.22±2.46	33.61±2.59	67.15±0.42	60.71±3.05	15.64±0.32	**61.11±2.62**	59.83±1.83
DCMVC + Hungarian	27.63±1.07	16.49±1.72	22.27±1.69	60.41±0.47	29.39±0.68	12.99±0.31	20.68±0.19	16.65±0.20
LMTC	57.39±2.89	40.01±4.69	33.29±3.81	58.75±0.55	45.75±0.55	23.24±0.45	24.01±0.25	47.31±0.25
LMTC + Hungarian	57.79±3.67	43.85±2.17	37.60±2.84	58.98±0.97	37.95±0.58	23.16±0.58	24.59±0.87	47.02±2.49
TMSL	28.68±1.25	12.02±1.10	23.71±1.08	69.33±0.61	48.62±0.54	21.34±0.36	OOM	OOM
TMSL + Hungarian	**68.40±1.91**	31.68±0.92	25.28±0.81	69.46±0.58	28.16±0.07	19.77±0.27	OOM	OOM
DSTL	39.59±1.18	37.00±0.00	23.41±1.99	60.53±0.55	29.05±0.50	15.54±0.33	11.64±0.22	20.40±0.15
DSTL + Hungarian	41.17±1.62	40.46±0.38	24.58±1.13	54.13±0.51	26.08±0.23	14.05±0.50	15.32±0.29	42.34±0.00
Ours	**69.31±1.32**	**61.20±0.83**	**70.28±0.55**	**85.34±0.42**	**92.09±0.00**	**30.27±0.20**	**74.84±0.94**	**75.50±0.14**

5.2 Compared Methods

Ten state-of-the-art MVC methods are selected as baselines for comparison, including EEOMVC [39], DealMVC [40], MVCAN [41], EBMGC [42], Vsc_mH [43], OpVuC [44], DCMVC [45], LMTC [46], TMSL [47], DSTL [48]. The detailed introductions of them are presented in Appendix A.5.

5.3 Experiments Setup

In the experiments, four widely used evaluation metrics are employed to assess the clustering performance of all compared methods: Accuracy (ACC), Normalized Mutual Information (NMI), Adjusted Rand Index (ARI), and F1score. For the proposed method, we conducted a grid search over the set $\{0.001, 0.01, 0.1, 1, 10, 100, 1000, 10000\}$ to determine the best value for each dataset. The unified latent feature dimension d is set to the number of clusters. Regarding the baseline methods, parameters were tuned according to the ranges provided in their respective publicly available source codes, and the best results were selected in the experiments. To mitigate the influence of randomness on the experimental results, each experiment was repeated 20 times, and the mean and variance of the results are reported. All experiments are conducted on a Windows 11 PC equipped with an Intel Core i7-13700F CPU and 64GB RAM.

5.4 Results Analysis

To facilitate a fair comparison between the proposed method and existing approaches under the sample non-alignment setting, we fix the sample alignment ratio ρ to 50% in the main experiments.

Table 3: ARI comparison of all methods with and without Hungarian alignment on eight multi-view datasets under a sample alignment ratio $\rho = 50\%$.

Method	Yale	3sources	MSRCV	100leaves	HW	Scene	EMNIST	Hdigit
EEOMVC	38.19±0.00	29.79±0.00	46.02±0.00	37.47±0.00	**86.99±0.00**	7.76±0.00	18.37±0.00	53.61±0.00
EEOMVC + Hungarian	32.46±0.00	21.51±0.00	45.98±0.00	36.53±0.00	32.12±0.00	6.93±0.00	16.33±0.00	42.83±0.00
DealMVC	11.75±0.00	2.51±0.44	4.49±1.72	1.89±0.25	21.77±1.06	6.57±0.91	23.83±1.59	38.45±1.65
DealMVC + Hungarian	3.35±0.00	0.24±0.61	3.49±0.21	2.61±0.49	18.77±1.58	8.98±2.30	15.57±0.49	**65.76±1.81**
MVCAN	10.54±1.71	4.92±1.55	35.98±2.09	30.37±1.53	22.24±0.58	16.37±0.60	16.49±0.38	50.04±3.04
MVCAN + Hungarian	11.10±1.07	29.57±4.45	24.14±3.45	20.57±1.66	30.14±5.39	12.52±0.10	29.21±12.52	42.30±4.52
EBMGC	15.43±0.00	12.29±0.00	14.78±0.00	15.36±0.00	31.06±0.00	5.75±0.00	12.37±0.00	22.04±0.00
EBMGC + Hungarian	9.89±0.00	13.21±0.00	17.44±0.00	15.36±0.00	24.43±0.00	8.60±0.00	15.06±0.00	36.00±0.00
Vsc_mH	37.27±0.00	36.47±0.00	45.47±0.00	23.39±0.00	20.92±0.00	13.26±0.00	24.93±0.00	46.54±0.00
OpVuC	30.40±0.00	33.68±0.00	5.49±0.00	40.64±0.00	10.90±0.00	15.39±0.00	34.32±0.00	38.69±0.00
DCMVC	4.69±1.05	19.77±5.08	19.55±2.22	29.23±0.91	53.01±2.79	8.81±0.24	48.53±3.72	49.42±2.03
DCMVC + Hungarian	2.01±0.84	4.26±1.13	14.93±1.54	19.50±0.73	24.12±0.73	6.88±0.24	15.51±0.57	12.12±0.22
LMTC	32.32±3.88	28.15±4.27	24.59±3.88	17.24±0.81	39.20±0.97	11.48±0.43	15.42±0.64	40.59±0.35
LMTC + Hungarian	32.71±4.91	30.32±2.02	27.45±3.00	17.58±1.45	19.07±1.17	11.26±0.43	15.09±0.78	37.54±2.25
TMSL	2.64±1.05	8.57±1.75	15.62±0.83	31.41±1.15	37.67±0.77	10.85±0.31	OOM	OOM
TMSL + Hungarian	47.94±3.13	32.77±1.34	16.48±0.77	31.38±1.02	23.93±0.06	9.99±0.21	OOM	OOM
DSTL	11.47±1.26	24.19±0.00	12.68±2.02	18.49±0.77	20.12±0.37	6.11±0.20	7.25±0.22	15.17±0.08
DSTL + Hungarian	13.70±2.01	37.03±0.36	14.86±0.97	11.85±0.71	18.22±0.36	5.44±0.25	9.31±0.21	29.22±0.00
Ours	**48.91±2.65**	**45.98±1.61**	**66.34±0.66**	**59.97±0.95**	**92.49±0.00**	**17.15±0.32**	**65.52±2.12**	65.53±0.43

Table 4: F1score comparison of all methods with and without Hungarian alignment on eight multi-view datasets under a sample alignment ratio $\rho = 50\%$.

Method	Yale	3sources	MSRCV	100leaves	HW	Scene	EMNIST	Hdigit
EEOMVC	42.10±0.00	44.77±0.00	53.93±0.00	38.17±0.00	88.29±0.00	15.02±0.00	28.53±0.00	58.97±0.00
EEOMVC + Hungarian	36.75±0.00	36.99±0.00	53.83±0.00	37.28±0.00	41.02±0.00	14.41±0.00	26.56±0.00	49.21±0.00
DealMVC	25.78±0.00	31.29±1.10	26.27±2.57	6.68±0.15	32.01±0.87	14.88±0.95	32.84±1.17	44.73±1.50
DealMVC + Hungarian	23.89±0.00	30.27±2.35	25.19±1.20	7.66±1.06	30.95±1.94	18.86±1.72	27.34±0.04	**69.41±1.61**
MVCAN	25.09±1.61	29.14±1.02	47.00±1.67	37.49±1.29	34.95±0.45	22.78±0.41	25.18±0.26	57.33±1.99
MVCAN + Hungarian	25.35±1.43	54.48±2.79	37.97±2.34	28.31±1.85	39.76±3.43	19.98±0.15	37.12±11.11	49.72±3.79
EBMGC	20.59±0.00	29.02±0.00	26.60±0.00	16.16±0.00	37.92±0.00	12.13±0.00	21.13±0.00	29.84±0.00
EBMGC + Hungarian	15.38±0.00	29.77±0.00	28.90±0.00	16.16±0.00	31.95±0.00	14.80±0.00	23.55±0.00	42.40±0.00
Vsc_mH	41.70±0.00	52.20±0.00	53.91±0.00	24.41±0.00	29.42±0.00	20.55±0.00	32.83±0.00	51.99±0.00
OpVuC	34.92±0.00	46.62±0.00	20.44±0.00	41.36±0.00	20.65±0.00	21.59±0.00	41.09±0.00	44.99±0.00
DCMVC	19.48±0.98	41.10±2.31	35.18±1.69	35.08±0.61	59.95±3.01	15.57±0.23	55.15±3.28	56.02±2.45
DCMVC + Hungarian	17.08±0.81	36.92±1.97	30.19±1.32	25.58±0.63	33.17±0.62	13.94±0.19	25.51±0.33	21.22±0.23
LMTC	36.59±3.61	42.40±3.28	35.28±3.33	18.07±0.81	45.29±0.87	17.65±0.41	24.48±0.42	46.62±0.31
LMTC + Hungarian	36.95±4.57	43.81±1.57	37.70±2.54	18.41±1.43	29.32±0.89	17.43±0.40	24.34±0.42	43.94±2.04
TMSL	9.04±0.97	32.77±2.01	27.43±0.74	32.09±1.14	44.06±0.68	17.46±0.34	OOM	OOM
TMSL + Hungarian	51.19±2.91	47.76±1.06	28.15±0.67	32.07±1.01	31.54±0.06	16.37±0.20	OOM	OOM
DSTL	17.50±1.09	47.67±0.00	25.27±1.75	19.35±0.75	28.38±0.35	12.65±0.20	16.81±0.16	23.70±0.07
DSTL + Hungarian	19.25±1.87	51.00±0.28	26.87±0.84	12.79±0.71	26.72±0.34	12.06±0.24	18.65±0.22	37.49±0.00
Ours	**52.17±2.43**	**56.59±1.34**	**71.03±0.57**	**60.37±0.94**	**93.24±0.00**	**22.94±0.29**	**69.12±1.85**	69.16±0.37

Due to space constraints, results under other alignment ratios are provided in the Appendix and can be found in Tables 7-8 for reference. Notably, some baselines are not directly applicable to the non-aligned scenario. For fair evaluation, we apply the Hungarian algorithm to align the data before using these methods. Clustering results under the four evaluation metrics are shown in Tables 1-4 with the best and the second results highlighted in **bold** and underlined respectively. Methods that encounter memory overflow are marked as OOM. Based on the results reported in the Tables, several key observations can be obtained:

(1) The proposed algorithm consistently outperforms most baseline methods, including those using Hungarian-based sample alignment. For example, on the EMNIST and MSRCV datasets, it achieves ACC improvements of 10.66% and 17.83% over the second-best methods, EEOMVC and DCMVC, respectively. Similar gains are observed across other datasets, highlighting the method's effectiveness in capturing true cross-view sample correspondences and enhancing clustering performance.

(2) Our method is superior to existing methods such as Vsc_mH and OpVuC, which are designed for non-aligned sample clustering. These two kind of methods rely on mining alignment relationships directly from raw features without explicitly modeling the structural hierarchy within each view. Moreover, they employ a hard matching strategy, determining class correspondences based on pairwise sample similarity. Due to high intra-class similarity, this often results in unstable alignment matrices, adversely affecting algorithm convergence and leading to performance fluctuations.

(3) Compared with deep clustering methods such as DealMVC, MVCAN, and DCMVC, the proposed method demonstrates notable advantages. Although deep neural networks possess strong representation capabilities, they often rely on the assumption of consistent semantic information

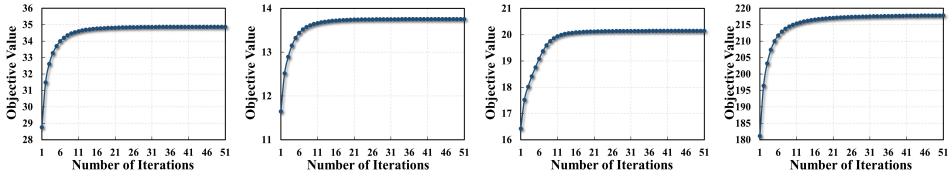

(a) Yale (b) 3sources (c) MSRCV (d) 100leaves

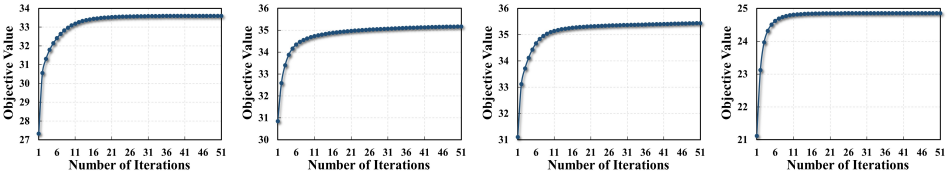

(e) HW (f) Scene (g) EMNIST (h) Hdigit

Figure 2: The objective function values of the proposed method across iterations.

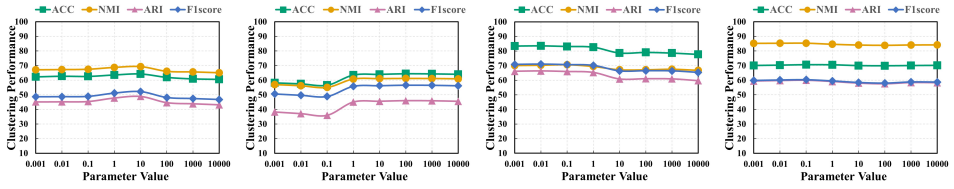

(a) Yale (b) 3sources (c) MSRCV (d) 100leaves

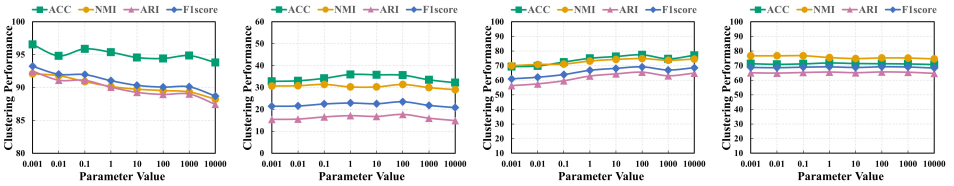

(e) HW (f) Scene (g) EMNIST (h) Hdigit

Figure 3: Clustering performance of the proposed method with varying values of the parameter λ.

across views. This assumption breaks down in the presence of sample misalignment, resulting in inconsistent feature learning and diminished clustering performance. Moreover, the use of the Hungarian algorithm for late fusion alignment does not consistently lead to performance gains and can even degrade results. This may be due to incorrect alignments introducing noisy or misleading information, ultimately impairing the effectiveness of the model.

5.5 Convergence and Parameter Sensitivity Analysis

In the previous section, we theoretically established that the proposed algorithm converges within a finite number of iterations. In this section, we further verify the convergence behavior empirically. The corresponding experimental results are illustrated in Fig. 2. As shown in the figure, the proposed method typically converges within approximately 10 iterations across all datasets, which empirically confirms its favorable convergence properties.

The results of our proposed method across varying λ values are presented in Fig. 3. Overall, the method demonstrates strong robustness to λ, with stable performance on most datasets. Notably, fluctuations on datasets like 3sources suggest higher sensitivity, may be can attributed to significant semantic divergence among views, which underscores the importance of appropriately weighting structural similarity.

5.6 Ablation Studies

We conduct ablation studies to assess the contribution of the proposed cross-view structural similarity module to clustering performance. Specifically, we denote the model without this module as SSA-MVC w/o CVS. The results, shown in Fig. 4, indicate that incorporating the module consistently improves sample alignment and clustering performance across most datasets. These findings highlight the effectiveness of the module and its integral role in the overall framework.

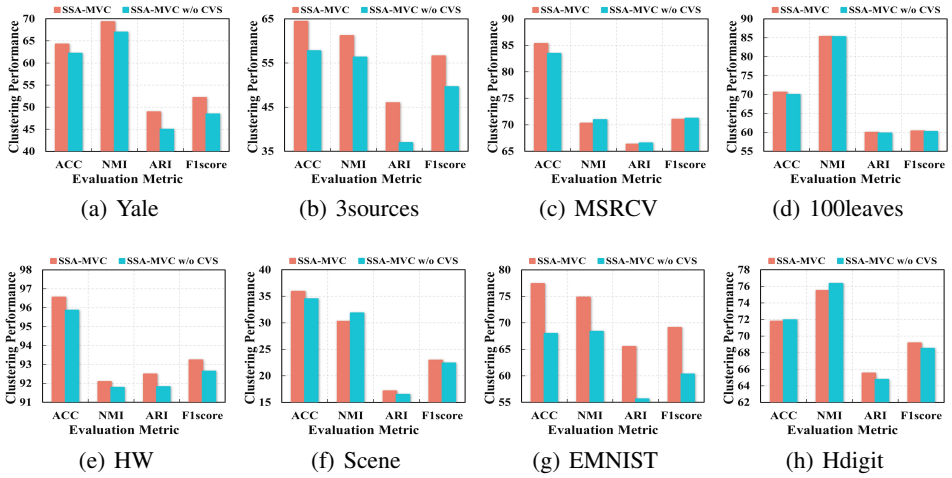

(a) Yale (b) 3sources (c) MSRCV (d) 100leaves

(e) HW (f) Scene (g) EMNIST (h) Hdigit

Figure 4: Clustering performance of the proposed method and its variant on eight multi-view datasets.

5.7 Effectiveness of the Alignment Strategy

To evaluate the scalability of our proposed method, we assess its effectiveness on the clustering algorithms that do not inherently handle sample misalignment. Specifically, under an alignment ratio of $\rho = 50\%$, we use $\mathbf{M}$ to realign the originally non-aligned 100leaves multi-view data and compare the performance of several baseline algorithms on both the original and the realigned 100leaves. As shown in Table 5, our method can benefit the clustering performance of these algorithms in the non-aligned setting, demonstrating its effectiveness and potential for generalization to other methods.

Table 5: Results of competitors on the 100leaves under a sample alignment ratio of $\rho = 50\%$.

Setting	Metric	DealMVC	MVCAN	EBMGC	DCMVC	LMTC	TMSL	DSTL
ACC	Unaligned	7.69±0.00	**49.51±1.24**	33.94±0.00	48.83±0.83	35.58±0.94	47.47±1.40	**36.87±1.42**
	Aligned+Ours	**12.42±0.52**	48.81±1.28	**43.06±0.00**	**53.75±0.89**	**40.82±1.31**	**48.18±1.37**	35.60±0.90
NMI	Unaligned	25.34±0.44	69.50±0.95	58.22±0.00	67.15±0.42	58.75±0.55	69.33±0.61	60.53±0.55
	Aligned+Ours	**38.01±0.46**	**69.95±0.59**	**64.52±0.00**	**72.10±0.49**	**64.58±0.80**	**70.54±0.57**	**61.09±0.53**
ARI	Unaligned	1.89±0.25	30.37±1.53	15.36±0.00	29.23±0.91	17.24±0.81	31.41±1.15	18.49±0.77
	Aligned+Ours	**5.16±0.12**	**30.58±0.99**	**24.62±0.00**	**36.50±0.87**	**24.46±1.24**	**32.67±1.17**	**19.38±0.68**
F1score	Unaligned	6.68±0.15	37.49±1.29	16.16±0.00	35.08±0.61	18.07±0.81	32.09±1.14	19.35±0.75
	Aligned+Ours	**11.47±0.14**	**37.74±0.93**	**25.33±0.00**	**41.38±0.85**	**25.21±1.23**	**33.34±1.15**	**20.23±0.67**

6 Conclusion

This paper proposes a scalable multi-view clustering algorithm to tackle sample non-alignment. By selecting a baseline view via the CLM algorithm and leveraging structural similarities between aligned and non-aligned samples, the method guides cross-view alignment and integrates the resulting alignment matrix into a late fusion clustering framework. Experiments on eight benchmark datasets validate the effectiveness of the proposed method.

Acknowledgments

This work was supported by the National Natural Science Foundation of China (NO. 62325604, 62276271, 62441618).

References

[1] Yingming Li, Ming Yang, and Zhongfei Zhang. A survey of multi-view representation learning. *IEEE transactions on knowledge and data engineering*, 31(10):1863–1883, 2018.

[2] Uno Fang, Man Li, Jianxin Li, Longxiang Gao, Tao Jia, and Yanchun Zhang. A comprehensive survey on multi-view clustering. *IEEE Transactions on Knowledge and Data Engineering*, 35(12):12350–12368, 2023.

[3] Cai Xu, Jiajun Si, Ziyu Guan, Wei Zhao, Yue Wu, and Xiyue Gao. Reliable conflictive multi-view learning. In *Proceedings of the AAAI conference on artificial intelligence*, volume 38, pages 16129–16137, 2024.

[4] Xinhang Wan, Bin Xiao, Xinwang Liu, Jiyuan Liu, Weixuan Liang, and En Zhu. Fast continual multi-view clustering with incomplete views. *IEEE Transactions on Image Processing*, 33:2995–3008, 2024.

[5] Hao Yu, Weixuan Liang, Ke Liang, Suyuan Liu, Meng Liu, and Xinwang Liu. On the adversarial robustness of multi-kernel clustering. In *Forty-second International Conference on Machine Learning*.

[6] Steffen Bickel and Tobias Scheffer. Multi-view clustering. In *ICDM*, volume 4, pages 19–26. Citeseer, 2004.

[7] Mouxing Yang, Yunfan Li, Peng Hu, Jinfeng Bai, Jiancheng Lv, and Xi Peng. Robust multi-view clustering with incomplete information. *IEEE Transactions on Pattern Analysis and Machine Intelligence*, 45(1):1055–1069, 2022.

[8] Jun Wang, Zhenglai Li, Chang Tang, Suyuan Liu, Xinhang Wan, and Xinwang Liu. Multiple kernel clustering with adaptive multi-scale partition selection. *IEEE Transactions on Knowledge and Data Engineering*, 2024.

[9] Xinhang Wan, Jiyuan Liu, Xinbiao Gan, Xinwang Liu, Siwei Wang, Yi Wen, Tianjiao Wan, and En Zhu. One-step multi-view clustering with diverse representation. *IEEE Transactions on Neural Networks and Learning Systems*, pages 1–13, 2024.

[10] Weiqing Yan, Yuanyang Zhang, Chenlei Lv, Chang Tang, Guanghui Yue, Liang Liao, and Weisi Lin. Gcfagg: Global and cross-view feature aggregation for multi-view clustering. In *Proceedings of the IEEE/CVF conference on computer vision and pattern recognition*, pages 19863–19872, 2023.

[11] Zhenglai Li, Yuqi Shi, Xiao He, and Chang Tang. Mask-informed deep contrastive incomplete multi-view clustering. *IEEE Transactions on Circuits and Systems for Video Technology*, 2025.

[12] Shengju Yu, Suyuan Liu, Siwei Wang, Chang Tang, Zhigang Luo, Xinwang Liu, and En Zhu. Sparse low-rank multi-view subspace clustering with consensus anchors and unified bipartite graph. *IEEE Transactions on Neural Networks and Learning Systems*, 36(1):1438–1452, 2025.

[13] G Ayorkor Mills-Tettey, Anthony Stentz, and M Bernardine Dias. The dynamic hungarian algorithm for the assignment problem with changing costs. *Robotics Institute, Pittsburgh, PA, Tech. Rep. CMU-RI-TR-07-27*, 2007.

[14] Shao-Yuan Li, Yuan Jiang, and Zhi-Hua Zhou. Partial multi-view clustering. In *Proceedings of the AAAI conference on artificial intelligence*, volume 28, 2014.

[15] Mouxing Yang, Yunfan Li, Zhenyu Huang, Zitao Liu, Peng Hu, and Xi Peng. Partially view-aligned representation learning with noise-robust contrastive loss. In *Proceedings of the IEEE/CVF conference on computer vision and pattern recognition*, pages 1134–1143, 2021.

[16] Yazhou Ren, Xinyue Chen, Jie Xu, Jingyu Pu, Yonghao Huang, Xiaorong Pu, Ce Zhu, Xiaofeng Zhu, Zhifeng Hao, and Lifang He. A novel federated multi-view clustering method for unaligned and incomplete data fusion. *Information Fusion*, 108:102357, 2024.

[17] Yan Yang and Hao Wang. Multi-view clustering: A survey. *Big data mining and analytics*, 1(2):83–107, 2018.

[18] Yi Wen, Siwei Wang, Ke Liang, Weixuan Liang, Xinhang Wan, Xinwang Liu, Suyuan Liu, Jiyuan Liu, and En Zhu. Scalable incomplete multi-view clustering with structure alignment. In *Proceedings of the 31st ACM International Conference on Multimedia*, pages 3031–3040, 2023.

[19] Chuan Tang, Miaomiao Li, Jun Wang, Chang Tang, Jiahe Jiang, Tianyi Wang, En Zhu, and Xinwang Liu. Multi-view clustering via high-order bipartite graph learning and tensor low-rank representation. *IEEE Transactions on Knowledge and Data Engineering*, 2025.

[20] Huayi Tang and Yong Liu. Deep safe multi-view clustering: Reducing the risk of clustering performance degradation caused by view increase. In *Proceedings of the IEEE/CVF Conference on Computer Vision and Pattern Recognition*, pages 202–211, 2022.

[21] Hyeon Jeon, Michaël Aupetit, DongHwa Shin, Aeri Cho, Seokhyeon Park, and Jinwook Seo. Measuring the validity of clustering validation datasets. *IEEE Transactions on Pattern Analysis and Machine Intelligence*, 2025.

[22] Guangcan Liu, Zhouchen Lin, Shuicheng Yan, Ju Sun, Yong Yu, and Yi Ma. Robust recovery of subspace structures by low-rank representation. *IEEE transactions on pattern analysis and machine intelligence*, 35(1):171–184, 2012.

[23] Hao Wang, Yan Yang, and Bing Liu. Gmc: Graph-based multi-view clustering. *IEEE Transactions on Knowledge and Data Engineering*, 32(6):1116–1129, 2019.

[24] Weixuan Liang, Xinwang Liu, Sihang Zhou, Jiyuan Liu, Siwei Wang, and En Zhu. Robust graph-based multi-view clustering. In *Proceedings of the AAAI conference on artificial intelligence*, volume 36, pages 7462–7469, 2022.

[25] Wenhui Zhao, Guangfei Li, Haizhou Yang, Quanxue Gao, and Qianqian Wang. Embedded feature selection on graph-based multi-view clustering. In *Proceedings of the AAAI Conference on Artificial Intelligence*, volume 38, pages 17016–17023, 2024.

[26] Ke Liang, Lingyuan Meng, Hao Li, Jun Wang, Long Lan, Miaomiao Li, Xinwang Liu, and Huaimin Wang. From concrete to abstract: Multi-view clustering on relational knowledge. *IEEE Transactions on Pattern Analysis and Machine Intelligence*, 2025.

[27] Feiping Nie, Xiaoqian Wang, and Heng Huang. Clustering and projected clustering with adaptive neighbors. In *Proceedings of the 20th ACM SIGKDD international conference on Knowledge discovery and data mining*, pages 977–986, 2014.

[28] Siwei Wang, Xinwang Liu, En Zhu, Chang Tang, Jiyuan Liu, Jingtao Hu, Jingyuan Xia, and Jianping Yin. Multi-view clustering via late fusion alignment maximization. In *IJCAI*, pages 3778–3784, 2019.

[29] Shudong Huang, Yixi Liu, Yazhou Ren, Ivor W Tsang, Zenglin Xu, and Jiancheng Lv. Learning smooth representation for multi-view subspace clustering. In *Proceedings of the 30th ACM international conference on multimedia*, pages 3421–3429, 2022.

[30] Hua Wang, Feiping Nie, and Heng Huang. Multi-view clustering and feature learning via structured sparsity. In *International conference on machine learning*, pages 352–360. PMLR, 2013.

[31] Shirui Luo, Changqing Zhang, Wei Zhang, and Xiaochun Cao. Consistent and specific multi-view subspace clustering. In *Proceedings of the AAAI conference on artificial intelligence*, volume 32, 2018.

[32] Shengju Yu, Zhibing Dong, Siwei Wang, Xinhang Wan, Yue Liu, Weixuan Liang, Pei Zhang, Wenxuan Tu, and Xinwang Liu. Towards resource-friendly, extensible and stable incomplete multi-view clustering. In *Proceedings of the 41st International Conference on Machine Learning*, pages 57415–57440, 2024.

[33] Siwei Wang, Xinwang Liu, and En Zhu. Late fusion multi-view clustering via global and local alignment maximization. *arXiv preprint arXiv:2208.01198*, 2022.

[34] Xinwang Liu, Li Liu, Qing Liao, Siwei Wang, Yi Zhang, Wenxuan Tu, Chang Tang, Jiyuan Liu, and En Zhu. One pass late fusion multi-view clustering. In *International conference on machine learning*, pages 6850–6859. PMLR, 2021.

[35] Xinwang Liu, Xinzhong Zhu, Miaomiao Li, Lei Wang, Chang Tang, Jianping Yin, Dinggang Shen, Huaimin Wang, and Wen Gao. Late fusion incomplete multi-view clustering. *IEEE transactions on pattern analysis and machine intelligence*, 41(10):2410–2423, 2018.

[36] Siwei Wang, Xinwang Liu, Suyuan Liu, Jiaqi Jin, Wenxuan Tu, Xinzhong Zhu, and En Zhu. Align then fusion: Generalized large-scale multi-view clustering with anchor matching correspondences. *Advances in Neural Information Processing Systems*, 35:5882–5895, 2022.

[37] Jiaqi Jin, Siwei Wang, Zhibin Dong, Xinwang Liu, and En Zhu. Deep incomplete multi-view clustering with cross-view partial sample and prototype alignment. In *Proceedings of the IEEE/CVF conference on computer vision and pattern recognition*, pages 11600–11609, 2023.

[38] Shengju Yu, Siwei Wang, Yi Wen, Ziming Wang, Zhigang Luo, En Zhu, and Xinwang Liu. How to construct corresponding anchors for incomplete multiview clustering. *IEEE Transactions on Circuits and Systems for Video Technology*, 34(4):2845–2860, 2024.

[39] Jun Wang, Chang Tang, Zhiguo Wan, Wei Zhang, Kun Sun, and Albert Y Zomaya. Efficient and effective one-step multiview clustering. *IEEE Transactions on Neural Networks and Learning Systems*, 2023.

[40] Xihong Yang, Jin Jiaqi, Siwei Wang, Ke Liang, Yue Liu, Yi Wen, Suyuan Liu, Sihang Zhou, Xinwang Liu, and En Zhu. Dealmvc: Dual contrastive calibration for multi-view clustering. In *Proceedings of the 31st ACM international conference on multimedia*, pages 337–346, 2023.

[41] Jie Xu, Yazhou Ren, Xiaolong Wang, Lei Feng, Zheng Zhang, Gang Niu, and Xiaofeng Zhu. Investigating and mitigating the side effects of noisy views for self-supervised clustering algorithms in practical multi-view scenarios. In *Proceedings of the IEEE/CVF Conference on Computer Vision and Pattern Recognition*, pages 22957–22966, 2024.

[42] Danyang Wu, Zhenkun Yang, Jitao Lu, Jin Xu, Xiangmin Xu, and Feiping Nie. Ebmgc-gnf: Efficient balanced multi-view graph clustering via good neighbor fusion. *IEEE Transactions on Pattern Analysis and Machine Intelligence*, 2024.

[43] Wenhua Dong, Xiao-Jun Wu, Tianyang Xu, Zhenhua Feng, Sara Atito Ali Ahmed, Muhammad Awais, and Josef Kittler. View-shuffled clustering via the modified hungarian algorithm. *Neural Networks*, 179:106602, 2024.

[44] Wenhua Dong, Xiao-Jun Wu, Zhenhua Feng, Sara Atito Ali Ahmed, Muhammad Awais, and Josef Kittler. One-pass view-unaligned clustering. *IEEE Transactions on Multimedia*, 2024.

[45] Jinrong Cui, Yuting Li, Han Huang, and Jie Wen. Dual contrast-driven deep multi-view clustering. *IEEE Transactions on Image Processing*, 2024.

[46] Jiyuan Liu, Xinwang Liu, Chuankun Li, Xinhang Wan, Hao Tan, Yi Zhang, Weixuan Liang, Qian Qu, Yu Feng, Renxiang Guan, et al. Large-scale multi-view tensor clustering with implicit linear kernels. In *Proceedings of the IEEE/CVF Conference on Computer Vision and Pattern Recognition*, 2025.

[47] Bing Cai, Gui-Fu Lu, Guangyan Ji, and Yangfan Du. Tensor multi-subspace learning for robust tensor-based multi-view clustering. *Knowledge-Based Systems*, page 113476, 2025.

[48] Deng Xu, Chao Zhang, Zechao Li, Chunlin Chen, and Huaxiong Li. Fast disentangled slim tensor learning for multi-view clustering. *IEEE Transactions on Multimedia*, 27:1254–1265, 2025.

[49] Yijie Lin, Yuanbiao Gou, Zitao Liu, Boyun Li, Jiancheng Lv, and Xi Peng. Completer: Incomplete multi-view clustering via contrastive prediction. In *Proceedings of the IEEE/CVF conference on computer vision and pattern recognition*, pages 11174–11183, 2021.

A Appendix

A.1 Limitations

As revealed by the construction process of the view-specific structural representations, the proposed method exhibits certain limitations when applied to scenarios where samples across views are completely unaligned. In such cases, a feasible approach is to explore the cross-view structural correlations by computing similarities between all samples in the to-be-aligned view and those in a designated baseline view. This cross-view relational information can then be integrated into the overall clustering framework after the main convergence process. Accordingly, future research will focus on designing multi-view clustering algorithms that are specifically tailored to handle fully unaligned sample scenarios.

A.2 The Pseudo Code of the Proposed Method

The detailed algorithm optimization processes are presented in the following.

Algorithm 1 The Algorithm of SSA-MVC.

Input: Unaligned multi-view data $\{\mathbf{X}^v\}_{v=1}^V$, the number of clusters k, the unified feature dimension d, and the hyper-parameter λ.
Construct the cross-view similarity graph $\{\mathbf{S}^v\}_{v=1}^V$ via Eqs. (3-(6)).
Initialize $\{\mathbf{R}^v\}_{v=1}^V$, $\{\mathbf{M}^v\}_{v=1}^V$, $\{\alpha_v\}_{v=1}^V$.
while not converge **do**
    Update $\mathbf{F}^*$ via Eq. (8).
    Update $\{\mathbf{R}^v\}_{v=1}^V$ via Eq. (10).
    Update $\{\alpha_v\}_{v=1}^V$ via Eq. (11).
    Update $\{\mathbf{M}^v\}_{v=1}^V$ via Eq. (13).
end while
Conduct k-means clustering algorithm on the consensus partition $\mathbf{F}^*$.
Output: Clustering results $\mathbf{Y}$.

A.3 Proof of Theorem 1

Proof. The proof can be divided into two parts, i.e., the objective function is upper bounded, and it is monotonically increasing.

1) The objective function is upper bounded.

Given that $\mathbf{M}^t = \mathbf{I}$, the overall objective function in Eq. (7) can be simplified as follows:

$$\begin{aligned} &\max_{\mathbf{R}^v, \mathbf{F}^*, \mathbf{M}^v, \alpha_v} \sum_{v=1}^{V} \mathrm{Tr}\big(\mathbf{F}^{*\top} \alpha_v \mathbf{C}^v \mathbf{F}^v \mathbf{R}^v\big) + \lambda \sum_{v=1}^{V} \mathrm{Tr}\big(\mathbf{M}^{v\top} \mathbf{S}^v\big) \\ &s.t.\ \mathbf{C}^v = \begin{bmatrix} \mathbf{I} & \mathbf{0} \\ \mathbf{0} & \mathbf{M}^v \end{bmatrix}, \mathbf{F}^{*\top}\mathbf{F}^* = \mathbf{I}, \mathbf{R}^{v\top}\mathbf{R}^v = \mathbf{I}, \sum_{v=1}^{V} \alpha_v^2 = 1, \mathbf{M}^{v\top}\mathbf{M}^v = \mathbf{I}. \end{aligned} \tag{14}$$

For any two distinct views v and v', where $v \neq v'$, the following inequality holds:

$$\begin{aligned} &\mathrm{Tr}\left((\alpha_v \mathbf{C}^v \mathbf{F}^v \mathbf{R}^v)^\top (\alpha_{v'} \mathbf{C}^{v'} \mathbf{F}^{v'} \mathbf{R}^{v'})\right) \\ &\leq \mathrm{Tr}\left((\mathbf{C}^v \mathbf{F}^v \mathbf{R}^v)^\top (\mathbf{C}^{v'} \mathbf{F}^{v'} \mathbf{R}^{v'})\right) \\ &\leq \frac{1}{2}\left(\mathrm{Tr}\left((\mathbf{C}^v \mathbf{F}^v \mathbf{R}^v)^\top (\mathbf{C}^v \mathbf{F}^v \mathbf{R}^v)\right) + \mathrm{Tr}\left((\mathbf{C}^{v'} \mathbf{F}^{v'} \mathbf{R}^{v'})^\top (\mathbf{C}^{v'} \mathbf{F}^{v'} \mathbf{R}^{v'})\right)\right) \\ &= d \end{aligned} \tag{15}$$

Based on the above inequality, we can further derive that:

$$\begin{aligned}
&\operatorname{Tr}\left(\mathbf{F}^{*\top}\sum_{v=1}^{V}\alpha_v\mathbf{C}^v\mathbf{F}^v\mathbf{R}^v\right)\\
&\leq\frac{1}{2}\left(\operatorname{Tr}(\mathbf{F}^{*\top}\mathbf{F}^*)+\operatorname{Tr}\left(\left(\sum_{v=1}^{V}\alpha_v\mathbf{C}^v\mathbf{F}^v\mathbf{R}^v\right)^{\top}\left(\sum_{v'=1}^{V}\alpha_{v'}\mathbf{C}^{v'}\mathbf{F}^{v'}\mathbf{R}^{v'}\right)\right)\right)\\
&\leq\frac{1}{2}(d+dn^2)
\end{aligned}\tag{16}$$

where d is the unified feature dimension, and n is the number of samples. Moreover, for the regularization term, we have:

$$\lambda\operatorname{Tr}(\mathbf{M}^{v\top}\mathbf{S}^v)\leq\frac{\lambda}{2}\left(\operatorname{Tr}(\mathbf{M}^{v\top}\mathbf{M}^v)+\operatorname{Tr}(\mathbf{S}^{v\top}\mathbf{S}^v)\right)=\frac{\lambda}{2}\left(n_2+\operatorname{Tr}(\mathbf{S}^{v\top}\mathbf{S}^v)\right)\tag{17}$$

where n_2 is a number of unaligned samples. Since $\operatorname{Tr}(\mathbf{S}^{v\top}\mathbf{S}^v)$ is a constant and λ is fixed, the term $\lambda\operatorname{Tr}(\mathbf{M}^{v\top}\mathbf{S}^v)$ is upper bounded.

Therefore, the overall objective function in Eq. (7) is guaranteed to be upper bounded.

2) The objective function is monotonically increasing.

In the aforementioned optimization procedure, it is apparent that the sub-problems involving the variables $\mathbf{F}^*$, $\mathbf{R}^v$, and $\mathbf{M}^v$ respectively, reduce to classical Orthogonal Procrustes Problems. Throughout the iterative solution process, the objective function values associated with these variables exhibit a monotonically non-decreasing trend. Additionally, the optimization with respect to the variable α constitutes a standard linear objective maximization problem under quadratic constraints, which similarly guarantees a monotonically non-decreasing progression of the objective value during updates. Let $\Theta(\mathbf{F}^*,\mathbf{M}^v,\mathbf{R}^v,\alpha_v)$ represent a simplified form of the objective function defined in Eq. (7). Thus, the following inequalities hold:

$$\Theta\big(\{\mathbf{F}^*\}^{(p)},\{\mathbf{M}^v\}^{(p)},\{\mathbf{R}^v\}^{(p)},\{\alpha_v\}^{(p)}\big)\leq\Theta\big(\{\mathbf{F}^*\}^{(p+1)},\{\mathbf{M}^v\}^{(p+1)},\{\mathbf{R}^v\}^{(p+1)},\{\alpha_v\}^{(p+1)}\big).\tag{18}$$

where the superscript (p) and $(p+1)$ denote the number of iterations.

Therefore, based on the aforementioned properties, we can conclude that the proposed algorithm is guaranteed to converge during the optimization process. □

A.4 Datasets Description

In our experiments, eight multi-view benchmark datasets are used to verify the effectiveness of our proposed method, including Yale[2], 3sources[3], MSRCV[4], 100leaves[5], HW[6], Scene [49], EMNIST[7], and Hdigit[8]. In the following, we will give a detailed introduction to them.

Yale: This dataset comprises 165 samples distributed across 15 distinct classes. Each sample is characterized by three heterogeneous feature sets: a 4096-dimensional Intensity descriptor, a 3304-dimensional Local Binary Pattern (LBP) descriptor, and a 6750-dimensional Gabor descriptor.

3sources: It comprises 169 samples collected from three distinct news media sources: BBC, Reuters, and The Guardian. Each sample is represented by three views, corresponding to the textual content extracted from each respective source. The feature dimensions for these views are 3560, 3631, and 3068 for BBC, Reuters, and The Guardian, respectively. All samples are annotated with one of six semantic classes.

[2]https://vision.ucsd.edu/content/yale-face-database

[3]http://mlg.ucd.ie/datasets/3sources.html

[4]https://mldta.com/dataset/msrc-v1/

[5]https://archive.ics.uci.edu/ml/datasets/Onehundred+plant+species+leaves+data+set

[6]https://archive.ics.uci.edu/ml/datasets/Multiple+Features

[7]https://www.nist.gov/itl/products-and-services/emnist-dataset

[8]https://cs.nyu.edu/ roweis/data.html

Table 6: Summary of eight benchmark multi-view datasets.

Datasets	#Classes	#Samples	#Views	#Feature Dimensionalities
Yale	15	165	3	4096; 3304; 6750
3sources	6	169	3	3560; 3631; 3068
MSRCV	7	210	5	24; 576; 512; 256; 254
100leaves	100	1600	3	64; 64; 64;
HW	10	2000	6	216; 76; 64; 6; 240; 47
Scene	15	4485	3	20; 59; 40
EMNIST	10	10000	4	576; 944; 512; 640
Hdigit	10	10000	2	784; 256

MSRCV: It comprises 210 image samples, each labeled with one of seven semantic classes. For each sample, a five-view feature representation is provided to capture diverse visual characteristics. Specifically, the dataset includes the following feature descriptors: 24-dimensional Color Moments (CM), 576-dimensional Histogram of Oriented Gradients (HOG), 512-dimensional GIST, 256-dimensional Local Binary Patterns (LBP), and 254-dimensional Gabor Energy-based Texture (GENT) features.

100leaves: The dataset comprises 1600 samples distributed across 100 distinct leaf species. Each sample is characterized by three complementary feature views: a 64-dimensional Texture Histogram (TH), a 64-dimensional Fourier Shape-based Metric (FSM), and a 64-dimensional Statistical Descriptor (SD). These multi-view features encapsulate diverse morphological and structural characteristics of the leaves, rendering the dataset highly suitable for the evaluation of multi-view learning and clustering algorithms.

HW: The dataset comprises 2000 samples, each annotated with one of ten distinct class labels. It encompasses six heterogeneous views, each representing diverse feature modalities extracted from the same set of samples. Specifically, these views include: 76-dimensional FOU features, 216-dimensional FAC features, 64-dimensional KAR features, 240-dimensional PIX features, 47-dimensional ZER features, and 6-dimensional MOR features.

Scene: The dataset comprises 4485 samples distributed across 15 distinct scene categories. Each sample is described by three complementary visual modalities: a 1800-dimensional GIST descriptor capturing the global spatial layout, a 1180-dimensional PHOG feature encoding local shape information, and a 1240-dimensional LBP representation characterizing texture patterns.

EMNIST: The dataset comprises 10000 samples distributed across 10 distinct classes. Each sample is characterized by four heterogeneous views, each providing complementary information derived from different feature sets. Specifically, the dimensionalities of the features corresponding to the four views are 576, 944, 512, and 640, respectively.

Hdigit: The dataset comprises 5000 handwritten digit images, representing the ten classes from 0 to 9. These samples are drawn from two distinct sources: the MNIST and USPS digit datasets. By integrating variations in handwriting styles and image resolutions inherent to both domains, the dataset offers a comprehensive and challenging benchmark for evaluating digit recognition algorithms.

A.5 Compared Methods Introduction

In this section, the specific introduction of ten state-of-the-art multi-view clustering methods is illustrated in the following.

EEOMVC (TNNLS 23) [39]: This method efficiently performs one-step multi-view clustering by constructing anchor-based similarity graphs to learn unified latent partition representations, enabling direct extraction of discrete clustering labels. By integrating latent information fusion and clustering into a joint framework, it significantly reduces computational complexity while improving clustering accuracy on large-scale datasets.

DealMVC(ACM MM 23) [40]: The proposed method addresses the limitation of existing multi-view clustering models by aligning similar yet distinct samples across views through dual contrastive

Table 7: Clustering performance of all compared methods on eight multi-view datasets under a sample alignment ratio of $\rho = 25\%$.

Dataset	Metric	EEOMVC	DealMVC	MVCAN	EBMGC	Vsc_mH	OpVuC	DCMVC	LMTC	TMSL	DSTL	Ours
Yale	ACC	47.88±0.00	10.30±0.00	26.18±1.94	27.27±0.00	43.64±0.00	24.24±0.00	22.91±1.04	47.55±3.35	22.21±1.13	30.27±1.45	63.70±2.15
	NMI	52.06±0.00	8.90±0.00	33.85±2.67	33.22±0.00	48.62±0.00	27.76±0.00	27.42±1.11	53.72±2.81	26.70±1.08	35.32±1.33	66.45±1.30
	ARI	27.86±0.00	0.00±0.00	5.96±1.82	5.51±0.00	20.60±0.00	2.12±0.00	1.71±0.70	27.03±3.46	0.93±0.68	7.68±1.12	45.33±2.21
	F1score	32.37±0.00	15.60±0.00	20.39±1.50	11.27±0.00	25.61±0.00	8.83±0.00	16.61±0.60	31.64±3.24	7.18±0.63	13.72±1.06	48.75±2.06
3sources	ACC	53.25±0.00	31.48±0.95	28.69±1.26	33.14±0.00	53.85±0.00	44.38±0.00	33.73±2.97	45.62±3.68	36.42±1.74	43.28±0.29	62.31±0.79
	NMI	29.93±0.00	4.76±0.17	9.24±2.28	13.84±0.00	33.23±0.00	25.19±0.00	15.43±2.18	33.76±5.62	5.84±0.73	20.33±0.56	55.65±0.18
	ARI	26.50±0.00	0.04±0.53	1.20±1.28	4.96±0.00	22.59±0.00	25.16±0.00	5.30±3.33	23.78±5.21	1.04±0.94	14.00±0.82	41.89±0.69
	F1score	41.65±0.00	31.68±0.90	27.21±1.47	23.09±0.00	46.29±0.00	40.12±0.00	34.09±3.03	38.77±4.29	30.37±1.17	40.04±0.16	53.24±0.58
MSRCV	ACC	60.95±0.00	33.62±2.48	49.62±6.05	26.67±0.00	55.24±0.00	26.67±0.00	39.95±2.33	47.40±2.12	32.29±0.63	35.88±3.02	80.12±0.43
	NMI	47.27±0.00	13.07±1.64	39.58±6.76	10.62±0.00	44.69±0.00	7.59±0.00	30.36±1.89	33.35±2.18	11.74±0.72	18.68±1.59	66.45±0.94
	ARI	37.21±0.00	6.00±2.03	25.61±5.75	3.37±0.00	33.00±0.00	3.21±0.00	15.15±1.82	21.43±1.78	5.04±0.33	9.57±1.38	61.49±0.83
	F1score	46.16±0.00	23.55±1.19	40.02±5.38	16.78±0.00	42.50±0.00	18.14±0.00	31.63±1.36	32.47±1.46	18.52±0.28	22.32±1.23	66.87±0.71
100leaves	ACC	39.69±0.00	4.14±0.15	29.93±0.89	21.44±0.00	24.69±0.00	18.50±0.00	31.82±0.60	22.92±0.96	43.50±0.92	22.23±0.76	66.51±0.92
	NMI	59.31±0.00	13.66±0.12	58.28±0.65	50.90±0.00	54.50±0.00	46.59±0.00	57.20±0.59	50.21±0.65	68.98±0.45	50.93±0.50	83.11±0.27
	ARI	19.07±0.00	0.19±0.04	13.66±0.70	6.24±0.00	11.50±0.00	6.67±0.00	15.35±0.79	7.93±0.85	29.30±0.97	7.38±0.43	55.29±0.91
	F1score	19.92±0.00	3.87±0.05	21.15±0.67	7.12±0.00	12.63±0.00	7.93±0.00	21.85±0.54	8.86±0.84	30.00±0.96	8.37±0.42	55.74±0.90
HW	ACC	92.05±0.00	27.58±0.84	28.55±0.03	20.80±0.00	19.25±0.00	19.20±0.00	75.25±1.67	45.59±2.36	60.67±0.48	31.56±0.66	96.35±0.00
	NMI	83.78±0.00	7.85±0.28	8.70±0.05	6.75±0.00	10.27±0.00	4.44±0.00	73.09±0.88	29.00±1.70	47.52±0.26	16.38±0.39	91.59±0.00
	ARI	83.22±0.00	4.96±0.54	5.06±0.03	3.37±0.00	1.55±0.00	1.85±0.00	65.60±1.36	21.06±1.75	37.85±0.40	9.85±0.30	92.08±0.00
	F1score	84.89±0.00	16.40±0.10	15.58±0.02	12.99±0.00	17.32±0.00	12.53±0.00	70.78±1.28	29.00±1.57	44.07±0.35	18.92±0.28	92.87±0.00
Scene	ACC	23.90±0.00	15.04±0.37	26.77±0.37	14.25±0.00	29.68±0.00	15.92±0.00	17.08±0.19	26.99±0.55	25.56±0.70	16.60±0.47	32.95±0.78
	NMI	16.45±0.00	3.48±0.13	30.82±0.62	3.76±0.00	28.68±0.00	6.26±0.00	5.64±0.26	22.17±0.39	18.65±0.49	10.07±0.22	27.79±0.32
	ARI	7.24±0.00	1.45±0.06	14.49±0.33	1.44±0.00	15.06±0.00	2.25±0.00	2.47±0.14	10.65±0.36	9.03±0.52	3.66±0.15	14.36±0.32
	F1score	14.41±0.00	10.70±0.21	21.28±0.27	8.12±0.00	21.56±0.00	10.48±0.00	9.72±0.14	16.87±0.34	15.81±0.54	10.52±0.16	20.35±0.29
EMNIST	ACC	36.53±0.00	43.29±1.86	26.72±0.48	17.46±0.00	47.66±0.00	46.69±0.00	59.61±3.04	30.30±0.43	OOM	19.69±0.18	75.43±4.25
	NMI	17.58±0.00	30.64±3.19	5.79±0.10	3.64±0.00	39.73±0.00	41.04±0.00	60.23±3.14	10.11±0.27	OOM	4.33±0.07	70.66±1.87
	ARI	11.10±0.00	22.02±2.45	3.91±0.12	1.90±0.00	27.02±0.00	28.33±0.00	48.39±3.30	6.99±0.20	OOM	2.28±0.05	61.67±3.56
	F1score	21.17±0.00	32.39±1.43	13.74±0.09	11.70±0.00	34.59±0.00	35.65±0.00	55.20±3.29	16.32±0.18	OOM	12.30±0.07	65.65±3.13
Hdigit	ACC	64.76±0.00	41.34±1.18	60.24±6.04	20.82±0.00	58.38±0.00	24.09±0.00	57.54±2.22	53.64±1.48	OOM	30.10±0.06	71.65±4.61
	NMI	71.68±0.00	15.96±1.27	55.53±3.46	5.09±0.00	48.48±0.00	6.22±0.00	55.37±0.97	45.56±2.18	OOM	11.77±0.05	74.87±1.00
	ARI	53.06±0.00	13.21±1.27	43.99±5.45	2.93±0.00	39.14±0.00	3.89±0.00	42.73±0.81	34.89±1.42	OOM	8.02±0.03	63.35±3.00
	F1score	58.55±0.00	21.94±1.09	51.04±4.18	12.63±0.00	45.36±0.00	13.71±0.00	50.69±1.05	41.56±1.29	OOM	17.26±0.03	67.28±2.59

calibration losses at both global and local levels. This approach effectively integrates cross-view feature similarity and reliable class information, enhancing clustering performance and robustness.

MVCAN (CVPR 24) [41]: MVCAN is a theoretically grounded deep multi-view clustering method designed to mitigate the impact of noisy views by allowing unshared parameters and inconsistent clustering predictions across views. It employs a two-level iterative optimization to enhance representation learning, achieving multi-view consistency, complementarity, and robustness to noise.

EBMGC (TPAMI 24) [42]: This method effectively leverages consistent neighbor information across multiple views through a novel Cross-view Good Neighbors Voting module, while a balanced regularization term based on the p-power function adapts clustering to diverse data distributions. By incorporating graph coarsening and an accelerated coordinate descent algorithm, this method achieves superior clustering performance with high efficiency.

Vsc_mH (Neural Networks 24) [43]: This method effectively addresses the View-shuffled Problem by simultaneously establishing cross-view correspondences through a global alignment and modified Hungarian algorithm, and performing clustering via matrix factorization. This integrated approach enables robust clustering on shuffled multi-view data with varying alignment ratios, supported by both theoretical convergence guarantees and strong empirical performance.

OpVuC (TMM 24) [44]: This method simultaneously addresses instance alignment and clustering within a unified framework, effectively handling fully unaligned multi-view data without relying on any pre-aligned samples. By leveraging a novel global-local alignment strategy grounded in geometric invariance and a relaxed k-means clustering approach, OpVuC robustly processes data at any alignment level, demonstrating superior performance across benchmark datasets.

DCMVC (TIP 24) [45]: This paper introduces a deep multi-view clustering network with a dual contrastive mechanism that simultaneously enhances inter-cluster separation and within-cluster compactness to learn clustering-friendly representations. By integrating dynamic cluster diffusion and neighbor-guided positive alignment losses, it effectively fuses multi-view features into discriminative consensus representations, achieving superior clustering performance.

LMTC (CVPR 25) [46]: This method removes the tensor rotation trick to avoid inadvertent label information and introduces a large-scale multi-view tensor clustering approach that incorporates pair-wise similarities via an implicit linear kernel. This results in an efficient, linear-complexity algorithm that effectively improves clustering performance without relying on sequential data order.

TMSL (KBS 25) [47]: This method enhances traditional tensor-based multi-view clustering by leveraging tensor low-rank representation to capture the intrinsic data structure, resulting in a more

Table 8: Clustering performance of all compared methods on eight multi-view datasets under a sample alignment ratio of $\rho = 75\%$.

Dataset	Metric	EEOMVC	DealMVC	MVCAN	EBMGC	Vsc_mH	OpVuC	DCMVC	LMTC	TMSL	DSTL	Ours
Yale	ACC	58.79±0.00	35.76±0.00	47.27±0.77	47.88±0.00	56.36±0.00	47.27±0.00	41.03±1.72	60.03±4.15	33.97±2.32	46.30±2.62	63.91±2.99
	NMI	61.44±0.00	41.67±0.00	51.80±1.08	51.58±0.00	58.05±0.00	49.86±0.00	45.07±1.46	62.21±3.24	39.04±1.76	49.02±1.63	67.88±1.77
	ARI	38.57±0.00	17.33±0.00	24.80±1.31	24.29±0.00	32.25±0.00	23.35±0.00	18.16±1.75	40.19±4.51	11.37±1.75	22.57±2.26	47.71±2.28
	F1score	42.49±0.00	30.62±0.00	37.90±0.62	28.92±0.00	36.94±0.00	28.43±0.00	32.71±1.65	43.94±4.21	17.35±1.67	27.71±2.03	51.02±2.12
3sources	ACC	65.09±0.00	30.30±0.24	43.59±2.54	42.60±0.00	63.31±0.00	53.25±0.00	63.31±5.91	50.33±1.44	52.60±2.17	54.44±0.00	65.24±0.26
	NMI	49.55±0.00	5.23±0.92	28.13±3.29	28.48±0.00	55.46±0.00	38.55±0.00	44.27±4.34	46.97±2.71	30.84±1.01	39.62±0.00	61.18±0.10
	ARI	42.19±0.00	0.63±0.32	15.37±3.61	14.74±0.00	45.45±0.00	34.65±0.00	43.53±7.34	33.37±2.94	20.06±0.98	22.53±0.00	48.46±0.30
	F1score	54.26±0.00	30.16±2.44	40.04±1.96	31.01±0.00	56.91±0.00	47.46±0.00	55.81±3.44	46.54±2.30	40.42±1.60	43.93±0.00	58.51±0.25
MSRCV	ACC	78.57±0.00	45.05±0.57	68.52±1.29	64.29±0.00	70.48±0.00	27.62±0.00	46.62±0.65	75.29±2.81	58.14±2.75	45.50±2.72	84.60±0.28
	NMI	65.84±0.00	34.36±1.00	51.18±1.30	49.27±0.00	59.39±0.00	9.97±0.00	40.64±1.09	58.63±2.83	42.54±1.89	30.44±1.18	75.16±0.60
	ARI	56.66±0.00	20.28±0.86	42.01±1.78	41.03±0.00	48.87±0.00	3.69±0.00	26.50±1.03	52.50±3.48	31.99±2.56	19.22±1.29	70.05±0.54
	F1score	62.92±0.00	39.20±0.57	53.13±1.40	49.21±0.00	56.35±0.00	19.06±0.00	40.23±1.02	59.15±2.99	41.62±2.17	30.88±1.08	74.25±0.46
100leaves	ACC	77.00±0.00	8.73±0.82	68.80±1.79	51.25±0.00	44.25±0.00	48.69±0.00	70.58±0.93	51.30±1.24	58.72±1.74	53.18±1.82	76.56±1.26
	NMI	83.41±0.00	32.66±2.33	81.15±0.61	68.93±0.00	75.27±0.00	77.08±0.00	81.38±0.34	70.69±0.53	76.63±0.71	73.14±0.71	88.30±0.45
	ARI	46.93±0.00	3.24±0.76	52.67±1.56	32.15±0.00	32.79±0.00	33.97±0.00	54.35±0.86	33.81±1.04	43.57±1.54	36.45±1.44	67.03±1.42
	F1score	47.56±0.00	9.99±0.56	58.45±1.33	32.79±0.00	33.70±0.00	34.87±0.00	59.17±0.66	34.47±1.03	44.13±1.52	37.11±1.42	67.36±1.40
HW	ACC	95.30±0.00	63.59±0.38	71.24±0.34	76.25±0.00	34.10±0.00	34.95±0.00	69.37±1.37	76.77±0.63	74.85±0.24	57.91±2.11	96.43±0.03
	NMI	90.30±0.00	51.73±0.10	56.46±0.52	61.10±0.00	24.75±0.00	14.90±0.00	58.26±0.65	60.76±1.37	54.29±0.21	43.45±0.84	91.84±0.05
	ARI	89.97±0.00	45.74±0.05	49.02±0.45	58.38±0.00	12.59±0.00	8.73±0.00	51.46±1.00	51.84±2.50	52.16±0.32	34.34±1.37	92.21±0.06
	F1score	90.96±0.00	53.09±0.34	57.57±0.51	62.53±0.00	23.01±0.00	18.59±0.00	58.38±0.58	56.98±2.06	56.93±0.29	40.98±1.24	92.99±0.06
Scene	ACC	32.69±0.00	27.42±1.38	37.77±0.68	33.65±0.00	30.35±0.00	30.84±0.00	35.59±0.48	32.70±1.60	33.96±0.01	25.94±0.57	37.52±0.87
	NMI	27.97±0.00	22.36±0.19	34.47±0.55	25.00±0.00	28.94±0.00	28.94±0.00	29.52±1.06	27.54±0.76	24.54±0.07	21.28±0.23	32.89±0.35
	ARI	12.97±0.00	11.28±0.87	19.40±0.46	15.36±0.00	14.79±0.00	14.82±0.00	18.55±0.84	14.74±0.62	14.68±0.07	9.69±0.21	18.18±0.53
	F1score	20.18±0.00	22.56±0.40	26.77±0.52	21.10±0.00	21.27±0.00	21.20±0.00	24.44±0.88	20.68±0.58	20.56±0.07	15.96±0.20	23.92±0.49
EMNIST	ACC	58.45±0.00	58.19±2.26	63.43±0.44	70.05±0.00	47.38±0.00	47.74±0.00	58.13±2.17	52.81±2.09	OOM	35.63±0.79	80.96±3.20
	NMI	50.65±0.00	42.51±0.43	43.23±0.96	51.38±0.00	38.72±0.00	42.64±0.00	59.26±1.65	36.67±0.32	OOM	21.03±0.70	77.94±1.29
	ARI	33.56±0.00	34.24±0.42	38.62±0.52	47.83±0.00	26.36±0.00	30.39±0.00	46.13±2.30	28.90±0.50	OOM	13.45±0.80	70.46±3.06
	F1score	41.32±0.00	42.58±0.29	45.48±0.63	53.05±0.00	34.07±0.00	37.58±0.00	53.66±1.97	36.11±0.44	OOM	22.43±0.66	73.48±2.69
Hdigit	ACC	67.76±0.00	75.68±5.89	78.29±4.98	97.62±0.00	62.80±0.00	50.65±0.00	81.65±4.55	67.61±0.90	OOM	54.84±1.14	78.80±0.05
	NMI	76.06±0.00	65.64±3.31	67.74±5.71	93.35±0.00	52.86±0.00	39.47±0.00	74.01±2.32	58.01±0.31	OOM	34.71±0.33	81.67±0.01
	ARI	58.19±0.00	62.98±5.52	62.55±6.30	94.78±0.00	43.47±0.00	29.69±0.00	68.76±4.81	51.71±0.57	OOM	28.86±0.59	73.73±0.01
	F1score	62.99±0.00	67.83±4.48	67.27±5.45	95.30±0.00	49.25±0.00	36.81±0.00	73.23±3.77	56.64±0.50	OOM	36.01±0.53	76.50±0.01

reliable and robust multi-subspace representation. Integrated into a unified framework solved via the augmented Lagrangian algorithm, TMSL can also serve as a versatile post-processing strategy to improve the performance of various existing TMVC methods.

DSTL (TMM 25) [48]: This method efficiently captures high-order correlations among multi-view latent semantic representations while disentangling semantic-related and unrelated components to reduce feature redundancy. By aligning semantic-related features across views through a consensus indicator, DSTL achieves scalable and robust multi-view clustering without relying on affinity graphs.

A.6 Experimental Results with Varying Sample Alignment Ratios

To further assess the effectiveness of the proposed algorithm under different sample alignment rates, experiments were also conducted at 25% and 75% alignment rates, with detailed results shown in Tables 7-8. The findings confirm that our proposed method consistently maintains superior performance compared to other approaches. These results collectively validate the robustness and effectiveness of our algorithm in handling sample misalignment scenarios.

NeurIPS Paper Checklist

1. **Claims**

   Question: Do the main claims made in the abstract and introduction accurately reflect the paper's contributions and scope?

   Answer: [Yes]

   Justification: The specific contributions of this paper can be found in the abstract and introduction sections.

   Guidelines:

   - The answer NA means that the abstract and introduction do not include the claims made in the paper.
   - The abstract and/or introduction should clearly state the claims made, including the contributions made in the paper and important assumptions and limitations. A No or NA answer to this question will not be perceived well by the reviewers.
   - The claims made should match theoretical and experimental results, and reflect how much the results can be expected to generalize to other settings.
   - It is fine to include aspirational goals as motivation as long as it is clear that these goals are not attained by the paper.

2. **Limitations**

   Question: Does the paper discuss the limitations of the work performed by the authors?

   Answer: [Yes]

   Justification: The limitations of this paper are presented in the Appendix A.1.

   Guidelines:

   - The answer NA means that the paper has no limitation while the answer No means that the paper has limitations, but those are not discussed in the paper.
   - The authors are encouraged to create a separate "Limitations" section in their paper.
   - The paper should point out any strong assumptions and how robust the results are to violations of these assumptions (e.g., independence assumptions, noiseless settings, model well-specification, asymptotic approximations only holding locally). The authors should reflect on how these assumptions might be violated in practice and what the implications would be.
   - The authors should reflect on the scope of the claims made, e.g., if the approach was only tested on a few datasets or with a few runs. In general, empirical results often depend on implicit assumptions, which should be articulated.
   - The authors should reflect on the factors that influence the performance of the approach. For example, a facial recognition algorithm may perform poorly when image resolution is low or images are taken in low lighting. Or a speech-to-text system might not be used reliably to provide closed captions for online lectures because it fails to handle technical jargon.
   - The authors should discuss the computational efficiency of the proposed algorithms and how they scale with dataset size.
   - If applicable, the authors should discuss possible limitations of their approach to address problems of privacy and fairness.
   - While the authors might fear that complete honesty about limitations might be used by reviewers as grounds for rejection, a worse outcome might be that reviewers discover limitations that aren't acknowledged in the paper. The authors should use their best judgment and recognize that individual actions in favor of transparency play an important role in developing norms that preserve the integrity of the community. Reviewers will be specifically instructed to not penalize honesty concerning limitations.

3. **Theory assumptions and proofs**

   Question: For each theoretical result, does the paper provide the full set of assumptions and a complete (and correct) proof?

   Answer: [Yes]

Justification: The detailed proof of Theorem 1 can refer to Appendix A.3.

Guidelines:

- The answer NA means that the paper does not include theoretical results.
- All the theorems, formulas, and proofs in the paper should be numbered and cross-referenced.
- All assumptions should be clearly stated or referenced in the statement of any theorems.
- The proofs can either appear in the main paper or the supplemental material, but if they appear in the supplemental material, the authors are encouraged to provide a short proof sketch to provide intuition.
- Inversely, any informal proof provided in the core of the paper should be complemented by formal proofs provided in appendix or supplemental material.
- Theorems and Lemmas that the proof relies upon should be properly referenced.

4. **Experimental result reproducibility**

   Question: Does the paper fully disclose all the information needed to reproduce the main experimental results of the paper to the extent that it affects the main claims and/or conclusions of the paper (regardless of whether the code and data are provided or not)?

   Answer: [Yes]

   Justification: The experimental results of all compared methods on eight multi-view datasets are presented in the experiments section. Furthermore, the source code will be released after the review.

   Guidelines:

   - The answer NA means that the paper does not include experiments.
   - If the paper includes experiments, a No answer to this question will not be perceived well by the reviewers: Making the paper reproducible is important, regardless of whether the code and data are provided or not.
   - If the contribution is a dataset and/or model, the authors should describe the steps taken to make their results reproducible or verifiable.
   - Depending on the contribution, reproducibility can be accomplished in various ways. For example, if the contribution is a novel architecture, describing the architecture fully might suffice, or if the contribution is a specific model and empirical evaluation, it may be necessary to either make it possible for others to replicate the model with the same dataset, or provide access to the model. In general. releasing code and data is often one good way to accomplish this, but reproducibility can also be provided via detailed instructions for how to replicate the results, access to a hosted model (e.g., in the case of a large language model), releasing of a model checkpoint, or other means that are appropriate to the research performed.
   - While NeurIPS does not require releasing code, the conference does require all submissions to provide some reasonable avenue for reproducibility, which may depend on the nature of the contribution. For example
     (a) If the contribution is primarily a new algorithm, the paper should make it clear how to reproduce that algorithm.
     (b) If the contribution is primarily a new model architecture, the paper should describe the architecture clearly and fully.
     (c) If the contribution is a new model (e.g., a large language model), then there should either be a way to access this model for reproducing the results or a way to reproduce the model (e.g., with an open-source dataset or instructions for how to construct the dataset).
     (d) We recognize that reproducibility may be tricky in some cases, in which case authors are welcome to describe the particular way they provide for reproducibility. In the case of closed-source models, it may be that access to the model is limited in some way (e.g., to registered users), but it should be possible for other researchers to have some path to reproducing or verifying the results.

5. **Open access to data and code**

Question: Does the paper provide open access to the data and code, with sufficient instructions to faithfully reproduce the main experimental results, as described in supplemental material?

Answer: [No]

Justification: The source code and data will be released after the whole double-blind review.

Guidelines:

- The answer NA means that paper does not include experiments requiring code.
- Please see the NeurIPS code and data submission guidelines (`https://nips.cc/public/guides/CodeSubmissionPolicy`) for more details.
- While we encourage the release of code and data, we understand that this might not be possible, so "No" is an acceptable answer. Papers cannot be rejected simply for not including code, unless this is central to the contribution (e.g., for a new open-source benchmark).
- The instructions should contain the exact command and environment needed to run to reproduce the results. See the NeurIPS code and data submission guidelines (`https://nips.cc/public/guides/CodeSubmissionPolicy`) for more details.
- The authors should provide instructions on data access and preparation, including how to access the raw data, preprocessed data, intermediate data, and generated data, etc.
- The authors should provide scripts to reproduce all experimental results for the new proposed method and baselines. If only a subset of experiments are reproducible, they should state which ones are omitted from the script and why.
- At submission time, to preserve anonymity, the authors should release anonymized versions (if applicable).
- Providing as much information as possible in supplemental material (appended to the paper) is recommended, but including URLs to data and code is permitted.

6. **Experimental setting/details**

   Question: Does the paper specify all the training and test details (e.g., data splits, hyperparameters, how they were chosen, type of optimizer, etc.) necessary to understand the results?

   Answer: [Yes]

   Justification: The details of our experimental settings about our proposed method and competitors are described in the experiments section.

   Guidelines:

   - The answer NA means that the paper does not include experiments.
   - The experimental setting should be presented in the core of the paper to a level of detail that is necessary to appreciate the results and make sense of them.
   - The full details can be provided either with the code, in appendix, or as supplemental material.

7. **Experiment statistical significance**

   Question: Does the paper report error bars suitably and correctly defined or other appropriate information about the statistical significance of the experiments?

   Answer: [Yes]

   Justification: The standard deviations of the experimental results are reported in the Tables.

   Guidelines:

   - The answer NA means that the paper does not include experiments.
   - The authors should answer "Yes" if the results are accompanied by error bars, confidence intervals, or statistical significance tests, at least for the experiments that support the main claims of the paper.
   - The factors of variability that the error bars are capturing should be clearly stated (for example, train/test split, initialization, random drawing of some parameter, or overall run with given experimental conditions).

- The method for calculating the error bars should be explained (closed form formula, call to a library function, bootstrap, etc.)
- The assumptions made should be given (e.g., Normally distributed errors).
- It should be clear whether the error bar is the standard deviation or the standard error of the mean.
- It is OK to report 1-sigma error bars, but one should state it. The authors should preferably report a 2-sigma error bar than state that they have a 96% CI, if the hypothesis of Normality of errors is not verified.
- For asymmetric distributions, the authors should be careful not to show in tables or figures symmetric error bars that would yield results that are out of range (e.g. negative error rates).
- If error bars are reported in tables or plots, The authors should explain in the text how they were calculated and reference the corresponding figures or tables in the text.

8. **Experiments compute resources**

   Question: For each experiment, does the paper provide sufficient information on the computer resources (type of compute workers, memory, time of execution) needed to reproduce the experiments?

   Answer: [Yes]

   Justification: The specific computer resources are introduced in the experimental settings.

   Guidelines:

   - The answer NA means that the paper does not include experiments.
   - The paper should indicate the type of compute workers CPU or GPU, internal cluster, or cloud provider, including relevant memory and storage.
   - The paper should provide the amount of compute required for each of the individual experimental runs as well as estimate the total compute.
   - The paper should disclose whether the full research project required more compute than the experiments reported in the paper (e.g., preliminary or failed experiments that didn't make it into the paper).

9. **Code of ethics**

   Question: Does the research conducted in the paper conform, in every respect, with the NeurIPS Code of Ethics `https://neurips.cc/public/EthicsGuidelines`?

   Answer: [Yes]

   Justification: We have carefully reviewed the NeurIPS Code of Ethics and confirmed that our research satisfies its principles.

   Guidelines:

   - The answer NA means that the authors have not reviewed the NeurIPS Code of Ethics.
   - If the authors answer No, they should explain the special circumstances that require a deviation from the Code of Ethics.
   - The authors should make sure to preserve anonymity (e.g., if there is a special consideration due to laws or regulations in their jurisdiction).

10. **Broader impacts**

    Question: Does the paper discuss both potential positive societal impacts and negative societal impacts of the work performed?

    Answer: [Yes]

    Justification: This paper aims to address the sample non-alignment problem in multi-view clustering. By addressing this problem, the work can lead to more accurate and robust data integration from diverse sources, which is beneficial in areas like healthcare, education, and social research.

    Guidelines:

    - The answer NA means that there is no societal impact of the work performed.

- If the authors answer NA or No, they should explain why their work has no societal impact or why the paper does not address societal impact.
- Examples of negative societal impacts include potential malicious or unintended uses (e.g., disinformation, generating fake profiles, surveillance), fairness considerations (e.g., deployment of technologies that could make decisions that unfairly impact specific groups), privacy considerations, and security considerations.
- The conference expects that many papers will be foundational research and not tied to particular applications, let alone deployments. However, if there is a direct path to any negative applications, the authors should point it out. For example, it is legitimate to point out that an improvement in the quality of generative models could be used to generate deepfakes for disinformation. On the other hand, it is not needed to point out that a generic algorithm for optimizing neural networks could enable people to train models that generate Deepfakes faster.
- The authors should consider possible harms that could arise when the technology is being used as intended and functioning correctly, harms that could arise when the technology is being used as intended but gives incorrect results, and harms following from (intentional or unintentional) misuse of the technology.
- If there are negative societal impacts, the authors could also discuss possible mitigation strategies (e.g., gated release of models, providing defenses in addition to attacks, mechanisms for monitoring misuse, mechanisms to monitor how a system learns from feedback over time, improving the efficiency and accessibility of ML).

11. **Safeguards**

    Question: Does the paper describe safeguards that have been put in place for responsible release of data or models that have a high risk for misuse (e.g., pretrained language models, image generators, or scraped datasets)?

    Answer: [NA]

    Justification: [NA]

    Guidelines:

    - The answer NA means that the paper poses no such risks.
    - Released models that have a high risk for misuse or dual-use should be released with necessary safeguards to allow for controlled use of the model, for example by requiring that users adhere to usage guidelines or restrictions to access the model or implementing safety filters.
    - Datasets that have been scraped from the Internet could pose safety risks. The authors should describe how they avoided releasing unsafe images.
    - We recognize that providing effective safeguards is challenging, and many papers do not require this, but we encourage authors to take this into account and make a best faith effort.

12. **Licenses for existing assets**

    Question: Are the creators or original owners of assets (e.g., code, data, models), used in the paper, properly credited and are the license and terms of use explicitly mentioned and properly respected?

    Answer: [Yes]

    Justification: All of the compared methods and uesed datasets are cited in our paper.

    Guidelines:

    - The answer NA means that the paper does not use existing assets.
    - The authors should cite the original paper that produced the code package or dataset.
    - The authors should state which version of the asset is used and, if possible, include a URL.
    - The name of the license (e.g., CC-BY 4.0) should be included for each asset.
    - For scraped data from a particular source (e.g., website), the copyright and terms of service of that source should be provided.

- If assets are released, the license, copyright information, and terms of use in the package should be provided. For popular datasets, `paperswithcode.com/datasets` has curated licenses for some datasets. Their licensing guide can help determine the license of a dataset.
- For existing datasets that are re-packaged, both the original license and the license of the derived asset (if it has changed) should be provided.
- If this information is not available online, the authors are encouraged to reach out to the asset's creators.

13. **New assets**

    Question: Are new assets introduced in the paper well documented and is the documentation provided alongside the assets?

    Answer: [NA]

    Justification: [NA]

    Guidelines:

    - The answer NA means that the paper does not release new assets.
    - Researchers should communicate the details of the dataset/code/model as part of their submissions via structured templates. This includes details about training, license, limitations, etc.
    - The paper should discuss whether and how consent was obtained from people whose asset is used.
    - At submission time, remember to anonymize your assets (if applicable). You can either create an anonymized URL or include an anonymized zip file.

14. **Crowdsourcing and research with human subjects**

    Question: For crowdsourcing experiments and research with human subjects, does the paper include the full text of instructions given to participants and screenshots, if applicable, as well as details about compensation (if any)?

    Answer: [NA]

    Justification: [NA]

    Guidelines:

    - The answer NA means that the paper does not involve crowdsourcing nor research with human subjects.
    - Including this information in the supplemental material is fine, but if the main contribution of the paper involves human subjects, then as much detail as possible should be included in the main paper.
    - According to the NeurIPS Code of Ethics, workers involved in data collection, curation, or other labor should be paid at least the minimum wage in the country of the data collector.

15. **Institutional review board (IRB) approvals or equivalent for research with human subjects**

    Question: Does the paper describe potential risks incurred by study participants, whether such risks were disclosed to the subjects, and whether Institutional Review Board (IRB) approvals (or an equivalent approval/review based on the requirements of your country or institution) were obtained?

    Answer: [NA]

    Justification: [NA]

    Guidelines:

    - The answer NA means that the paper does not involve crowdsourcing nor research with human subjects.
    - Depending on the country in which research is conducted, IRB approval (or equivalent) may be required for any human subjects research. If you obtained IRB approval, you should clearly state this in the paper.

- We recognize that the procedures for this may vary significantly between institutions and locations, and we expect authors to adhere to the NeurIPS Code of Ethics and the guidelines for their institution.
- For initial submissions, do not include any information that would break anonymity (if applicable), such as the institution conducting the review.

16. **Declaration of LLM usage**

    Question: Does the paper describe the usage of LLMs if it is an important, original, or non-standard component of the core methods in this research? Note that if the LLM is used only for writing, editing, or formatting purposes and does not impact the core methodology, scientific rigorousness, or originality of the research, declaration is not required.

    Answer: [NA]

    Justification: [NA]

    Guidelines:

    - The answer NA means that the core method development in this research does not involve LLMs as any important, original, or non-standard components.
    - Please refer to our LLM policy (`https://neurips.cc/Conferences/2025/LLM`) for what should or should not be described.